Report on the APMP.PR-S6:2012-2013 Supplementary Comparison of

Spectral Radiance from 250 nm to 2500 nm

Final report

(Approved by APMP TCPR on 30 August 2019,

Approved by CCPR WG-KC on 30 September 2019)

Participants: KRISS (Korea), NIM (China), and VNIIOFI (Russia)

Pilot laboratory: KRISS

Dong-Joo Shin[1], Seongchong Park[1], Dong-Hoon Lee[1], Dai Caihong [2], Wu Zhifeng[2], Wang Yanfei[2], Boris Khlevnoy[3], Maxim Solodilov [3], and Svetlana Kolesnikova.[3]

[1] *Korea Research Institute of Standards and Science (KRISS),*
267 Gajeong-Ro, Yuseong-Gu, Daejeon 34113, Republic of Korea
Email: djshin@kriss.re.kr

[2]*National Institute of Metrology (NIM)*
No. 18 Bei San Huan Dong Lu, 100029, Beijing, China
Email: daicaihong@nim.ac.cn

[3] *All-Russian Research Institute for Optical and Physical Measurements (VNIIOFI),*
Ozernaya 46, Moscow 119361, Russia
Email: khlevnoy-m4@vniiofi.ru

Abstract

Korea Research Institute of Standards and Science (KRISS), National Institute of Metrology (NIM), and All-Russian Research Institute for Optical and Physical Measurements (VNIIOFI) started an international comparison on the spectral radiance over the spectral region from 250 nm to 2500 nm in 2012 and completed all measurements in 2016. The aim of this comparison was to assess the equivalence of the spectral radiance scales between the three laboratories. This comparison was carried out according to the technical protocol listed in the KCDB under the identifier APMP.PR-S6. The difference from the Reference Value (RV) and its uncertainty of each participant of this comparison were calculated by using the relative difference model recommended by the Guidelines for CCPR Comparison Report Preparation. A method (Ratio Method) to calculate the difference from the RV and its uncertainty was proposed to eliminate the pilot effects involved in the relative difference model. In the Ratio Method, spectral radiance ratios to the pilot and geometric means were used to calculate the difference from the RV and its uncertainty of each participant. Results of this comparison analyzed using the Ratio Method showed that differences from the RV of all participants were within their uncertainties (k = 2) except a few wavelengths for each participant.

Report on the APMP.PR-S6:2012-2013 Supplementary Comparison of

Spectral Radiance from 250 nm to 2500 nm

Final report (27 December 2019)

Contents

1. Introduction

The Korea Research Institute of Standards and Science (KRISS), and National Institute of Metrology (NIM) , and All-Russian Research Institute for Optical and Physical Measurements (VNIIOFI) agreed in March 2012 to conduct an international comparison on spectral radiance over the spectral region from 250 nm to 2500 nm as an APMP supplementary comparison. The aim of this comparison was to assess the equivalence of the spectral radiance scales between the three laboratories. The comparison was started in January 2013 and carried out according to the technical protocol listed in the KCDB under the identifier APMP.PR-S6. KRISS was the pilot laboratory. Three tungsten strip lamps were used as comparison artifacts. The measurement sequence was KRISS → VNIIOFI → KRISS → NIM → KRISS. The comparison had been delayed due to problems of KRISS measurement system and all measurements were completed in June 2016.

Differences from the reference value (RV) of this comparison and their uncertainties were calculated in accordance with the Guidelines for CCPR Key Comparison Report Preparation [1]. In the relative difference model recommended in the Appendix A of Ref [1] and used in the Final Report of CCPR S1 [2], however, pilot measurement effect was remained in the relative difference from the RV and its uncertainty of each participant. A calculation method (Ratio Method, hereinafter) using spectral radiance ratios of participants to the pilot, instead of the relative spectral radiance difference, was proposed to calculate the difference from the RV and its uncertainty without any effect of the pilot. The details of the Ratio Method are described in Appendix A of this report. Ratio Method is similar to the data analysis used in the Final Report of CCPR K1.a [3] except the use of spectral radiance ratios instead of systematic factors. Spectral radiance ratios of participants to the pilot were more convenient than the relative spectral radiance differences for the calculation of the difference from the RV, and especially for the calculation of its uncertainty because relative uncertainties reported by participants could be used directly.

Comparison results showed that the differences from the RV and their uncertainties of participants calculated by using the Ratio Method were within their expanded uncertainties (k = 2) except a few wavelengths for each participant.

2. Organization of the comparison

2.1. Participants

Three NMIs took part in this comparison: KRISS (Korea), NIM (China), and VNIIOFI (Russia). KRISS was the pilot laboratory. Details of participants presented in Table 2-1.

Table 2-1. Details of participants.

Laboratory	Function	Person in Charge	Contact
Korea Research Institute of Standards and Science(KRISS), 267 Gajeong-Ro, Yuseong-Gu, Daejeon 34113, Korea	Pilot	Dong-Joo Shin	Tel: +82-42-868-5209 Fax: +82-42-868-5022 Email: djshin@kriss.re.kr
National Institute of Metrology (NIM) No. 18 Bei San Huan Dong Lu, 100029, Beijing, China		Dai Caihong	Tel: +86 10 64524813 Fax: +86 10 64218651 Email: daicaihong@nim.ac.cn
All-Russian Research Institute for Optical and Physical Measurements (VNIIOFI), Ozernaya 46, 119361 Moscow, Russia		Boris B. Khlevnoy	Tel: +7 (495) 437-29-88 Fax: +7 (495) 437-29-92 Email: khlevnoy-m4@vniiofi.ru

2.2. Form of the comparison

The comparison was organized as a star comparison and the measurement sequence was

KRISS (1st meas.) → VNIIOFI → KRISS (2nd meas.) → NIM → KRISS (3rd meas.).

Measurements were started in January 2013 and completed in June 2016. KRISS as the pilot collected measurement results from both participants, and received in September 2016 from NIM and in January 2017 from VNIIOFI. KRISS made pre-Draft-A related to the relative data in accordance with the CCPR guidelines [1], distributed it to participants, and received agreements from both participants in February 2017. All participants have agreed to Draft A-4 in April 2017. During the reviewing process from Darft A-1 to Draft A-4, no change in measurement data has occurred. Draft-B is the final version of the Draft A-4. The Draft B was submitted to APMP TCPR in April 2017 and the review results were received in August 2019. Draft B-2 was submitted to APMP TCPR on 30 August 2019 after considering the review results and approved by APMP TCPR on 30 August 2019.

2.3. Description of the artifacts

The artifacts were three tungsten strip lamps made by the Moscow Lamp factory (type: TRU 1100-2350). The artifacts were labeled as TRU-2350-12-04.91, TRU-2350-12-04.87, and TRU-2350-12-02.86. The spectral range of calibration was from 250 nm to 2500 nm. Details of lamps and measurement conditions are presented in Table 2-2.

Table 2-2. Details of lamps and measurement conditions**.**

	KRISS	VNIIOFI	KRISS	NIM	KRISS
Measurement date	Feb. ~ Mar. 2013	May ~ Jun. 2013	Jan. ~ Mar. 2014	May ~ Nov. 2014	Jan. 2015 ~ Jun. 2016
Type of Lamps	TRU-2350-12-04.91, TRU-2350-12-04.87, TRU-2350-12-02.86				
Spectral Range	250 nm ~ 2500 nm (27 wavelengths)				
Electrical condition	TRU-2350-12-04.91: 23.020 A (6.3 V) TRU-2350-12-04.87: 23.570 A (6.7 V) TRU-2350-12-02.86: 22.580 A (6.6 V)				
Strip size	2.8 mm x 20 mm				
Target area	0.6 mm (width) x 0.8 mm (height)				
Solid angle	0.008 sr				

Figure 2-1 shows a lamp used as the artifact and its dimensions. Figure 2-2 shows the schematic diagram of the lamp. The lamp has a wire pointer in the middle height of the tungsten strip. A small circular mark in the rear surface of the lamp was made by marking with black ink after grinding the surface at KRISS. The wire pointer and the mark were used to align the lamp to the optical axis of the measurement system by positioning the lamp for the laser beam coming along the optical axis to reach the mark through the end of the wire pointer.

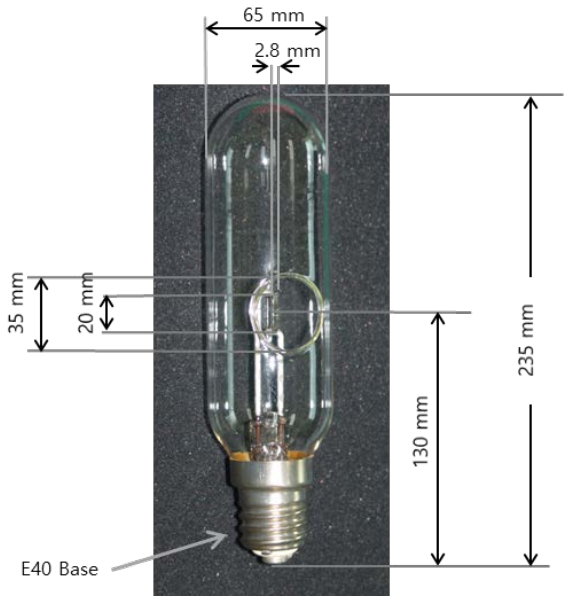

Figure 2-1. A tungsten strip lamp used as the artifact**.**

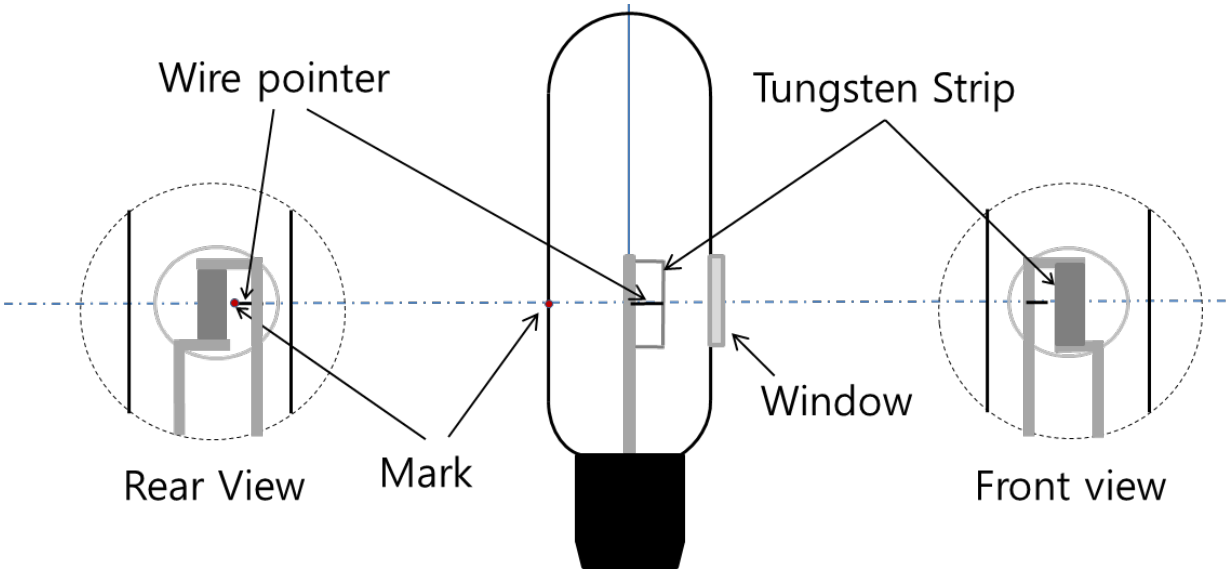

Figure 2-2. Schematic diagram of the lamp and the mark for alignment.

2.4. Spectral radiance of artifacts

As described in the protocol, the spectral radiances of lamps should be measured for two orthogonal polarizations. The spectral radiance of a lamp is given by

$$L_{\text{lamp}}(\lambda) = L_{\parallel,\text{lamp}}(\lambda) + L_{\perp,\text{lamp}} \tag{2-1}$$

where $L_{\text{lamp}}(\lambda)$ is the total spectral radiance of the lamp, and $L_{\parallel,\text{lamp}}(\lambda)$ and $L_{\perp,\text{lamp}}$ are spectral radiance components for two orthogonal polarizations.

When the lamp is calibrated by comparing with a blackbody, its spectral radiance is given by

$$L_{\text{lamp}}(\lambda) = \frac{1}{2} \cdot \left\{ R_{\parallel,\text{lamp,BB}}(\lambda) + R_{\perp,\text{lamp,BB}}(\lambda) \right\} \cdot L_{\text{BB}}(\lambda, T) \tag{2-2}$$

where $R_{\parallel,\text{lamp,BB}}(\lambda)$ and $R_{\perp,\text{lamp,BB}}(\lambda)$ are spectroradiometer signal ratios of a lamp to the blackbody for two orthogonal polarizations, respectively.

3. Measurements at KRISS

3.1. Description of measurement facility Spectral

The KRISS spectral radiance measurement facility is shown in Figure 3-1. In front of the blackbody, an aperture with a diameter of 3 mm was used as the reference plane of spectral radiance measurement. The diameter and position of the aperture was selected for the area of the radiator inside the blackbody imaged on the entrance surface of the spectroradiometer by the fore-optics[1] not to exceed the radiator diameter of 57 mm.

The fore-optics to make an image of the aperture in front of the blackbody and the tungsten strip of a lamp on the entrance surface of the spectroradiometer consists of a spherical mirror with a diameter of 100 mm and the radius of curvature of 1000 mm, and two flat mirrors. A mask was attached on the entrance surface of the spectroradiometer. The mask was made by laser machining of 50 μm thick stainless-steel and its size is 0.6 mm (wide) × 0.8 mm (high). A polarizer was used in front of the entrance surface to define two orthogonal polarizations of the incident beams. The polarizer was attached on a rotator and automatically controlled.

The spectroradiometer consists of a monochromator (McPherson Model 2061) with a prism predisperser,

[1] an input-optic of spectroradiometers which defines a measurement geometry such as field-of-view and f/#

and four detectors to cover the spectral range from 250 nm to 2500 nm. The focal length of the monochromator is 1 m and its numerical aperture is f/8.6. Three gratings with 600 grooves/mm blazed at 300 nm, 1000 nm, and 1800 nm were used for the wavelength range from 250 nm to 800 nm, from 800 nm to 1700 nm, and from 1700 nm to 2500 nm, respectively. The bandwidth of the spectroradiometer was set as 1.0 nm over the wavelength range from 250 nm to 800 nm and as 3.3 nm from 900 nm to 2500 nm.

Four detectors were used: a photomultiplier tube for the spectral range from 250 nm to 800 nm, a Si-photodiode from 800 nm to 1100 nm, an InGaAs detector from 1100 nm to 1700 nm, and an extended InGaAs detector from 1700 nm to 2500 nm. Gratings were manually exchanged and detectors were automatically exchanged according to the wavelength range.

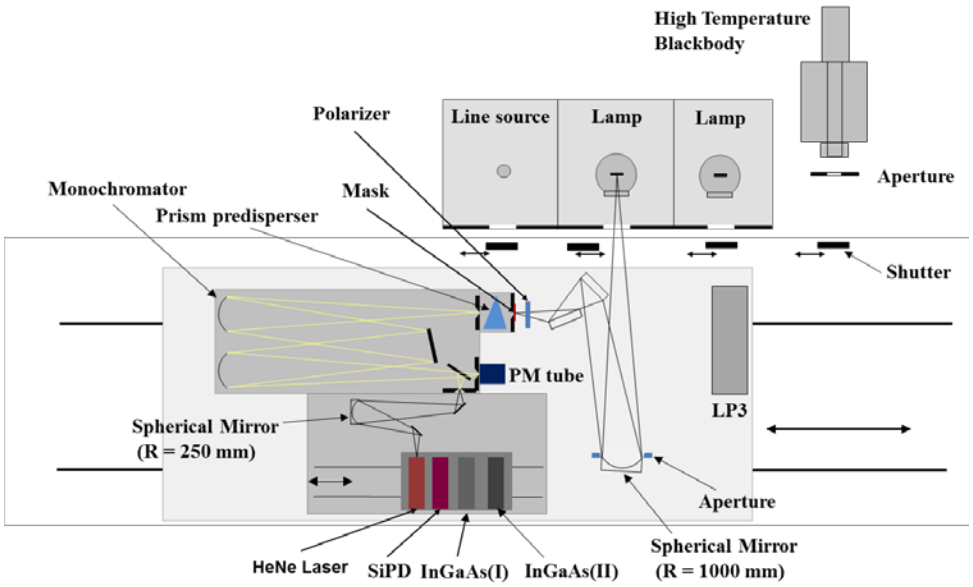

Figure 3-1. Spectral radiance measurement facility of KRISS.

3.2. Spectral radiance scale realization

The spectral radiance scale of KRISS was realized using a high-temperature blackbody (BB3500MP) made by VNIIOFI. The blackbody has a pyrolytic graphite radiator with a depth of 250 mm and a diameter of 57 mm, and has an opening diameter of 25 mm. The blackbody effective emissivity, estimated using a Monte-Carlo method calculation, was approximately 0.999 (see the section 5.2 for more details). The blackbody was operated at temperatures between 1800 K and 2400 K for this comparison. The temperature of the blackbody was measured using a radiation thermometer (LP3) calibrated by comparing the KRISS radiance temperature scale [4] based on ITS-90 [5]. The radiance temperature scale was realized by the same technique as used in CCT-K5. The blackbody temperature measurement uncertainty in this comparison was estimated to be 0.62 K (k = 1) including the KRISS radiance temperature scale uncertainty of 0.51 K.

The spectral radiance of the blackbody was given by

$$L_{\mathrm{BB}}(\lambda,T) = \varepsilon_{\mathrm{eff}} \cdot \frac{c_1}{\pi \cdot n^2 \cdot \lambda^5} \cdot \frac{1}{\exp\left(\frac{c_2}{n \cdot \lambda \cdot T}\right) - 1} \quad [\mathrm{W/(m^3 \cdot sr)}] \tag{3-1}$$

where
$c_1 = 3.741\,771\,18(19) \times 10^{-16}$ [W·m^2]
$c_2 = 1.438\,7752\,(25) \times 10^{-2}$ [m·K]
$n = 1.000285$ (air refractive index)
T: temperature of the blackbody
$\varepsilon_{\mathrm{eff}} = 0.999$ (effective emissivity of the blackbody).

The temperature of the blackbody was varied from about 1800 K to 2400 K depending on spectral ranges to match the spectral radiance of a tungsten strip lamp. Table 3-1 shows the uncertainty budget of the KRISS spectral radiance scale.

Table 3-1. Uncertainty budget of the spectral radiance scale realization at KRISS.

		Uncertainty Components				
		BB Temp Measurement	BB emissivity ε=0.999	Spatial uniformity at the aperture	Stability	Combined standard uncertainty (%)
	Wavelength (nm)	$u(T)$ = 0.62 K	$u(\varepsilon)$=0.001	$u(T)$ =0.18 K		(k=1)
1	250	0.61	0.10	0.18	0.10	**0.65**
2	260	0.59	0.10	0.17	0.10	**0.63**
3	270	0.57	0.10	0.16	0.09	**0.60**
4	280	0.54	0.10	0.16	0.09	**0.58**
5	290	0.53	0.10	0.15	0.09	**0.56**
6	300	0.51	0.10	0.15	0.08	**0.55**
7	325	0.47	0.10	0.14	0.08	**0.50**
8	350	0.44	0.10	0.13	0.07	**0.47**
9	375	0.45	0.10	0.12	0.07	**0.48**
10	400	0.42	0.10	0.11	0.07	**0.45**
11	450	0.37	0.10	0.10	0.06	**0.40**
12	500	0.34	0.10	0.09	0.05	**0.36**
13	550	0.30	0.10	0.08	0.05	**0.33**
14	600	0.28	0.10	0.07	0.05	**0.31**
15	656.3	0.26	0.10	0.07	0.04	**0.29**
16	700	0.24	0.10	0.06	0.04	**0.27**
17	800	0.21	0.10	0.06	0.03	**0.24**
18	900	0.19	0.10	0.05	0.03	**0.22**
19	1000	0.17	0.10	0.04	0.03	**0.20**
20	1050	0.16	0.10	0.04	0.03	**0.20**
21	1200	0.23	0.10	0.04	0.04	**0.25**
22	1550	0.18	0.10	0.03	0.03	**0.21**
23	1700	0.16	0.10	0.03	0.03	**0.19**
24	2100	0.13	0.10	0.02	0.02	**0.17**
25	2300	0.12	0.10	0.02	0.02	**0.16**
26	2400	0.12	0.10	0.02	0.02	**0.16**
27	2500	0.11	0.10	0.02	0.02	**0.15**

3.3. Laboratory conditions

The laboratory temperature was (23 ± 1) ºC and humidity was (65 ± 5) %.

3.4. Laboratory transfer standard

The artifacts were measured once by direct comparison with the blackbody and twice by comparing with a reference lamp. The reference lamp which is the same type was positioned between the blackbody and artifact. The reference lamp was calibrated by comparing with the blackbody when each lamp was calibrated by the blackbody. Then, the reference lamp was used to calibrate artifacts at the same position with no change.

3.5. Measurement of artifacts

3.5.1. Spectral radiance of artifacts

The artifacts were measured once by direct comparing with blackbody and twice by comparing with the reference lamp. The spectral radiance of an artifact was calculated as the average of three measurements. The spectroradiometer signal ratios between the artifact and the blackbody or the reference lamp at each wavelength was measured for two orthogonal polarizer orientations. The polarizer orientations were fixed. The spectral radiance of the artifact was calculated by

$$L_{\mathrm{lamp}}(\lambda) = \frac{1}{2} \cdot \left\{ R_{\parallel,\mathrm{lamp/BB}}(\lambda) + R_{\perp,\mathrm{lamp/BB}}(\lambda) \right\} \cdot L_{\mathrm{BB}}(\lambda, T) \tag{3-2}$$

when the lamp is calibrated by comparing with the blackbody. $R_{\parallel,\mathrm{lamp/BB}}(\lambda)$ and $R_{\perp,\mathrm{lamp/BB}}(\lambda)$ are signal ratios of the lamp to the blackbody for two orthogonal polarizer orientations, respectively. When the lamp is calibrated by comparing with the reference lamp, the spectral radiance of the lamp was calculated by

$$L_{\mathrm{lamp}}(\lambda) = R_{\parallel,\mathrm{lamp/ref}}(\lambda) \cdot L_{\parallel,\mathrm{ref}}(\lambda, T) + R_{\perp,\mathrm{lamp/ref}}(\lambda) \cdot L_{\perp,\mathrm{ref}}(\lambda, T) \tag{3-3}$$

where $R_{\parallel,\mathrm{lamp/ref}}(\lambda)$ and $R_{\perp,\mathrm{lamp/ref}}(\lambda)$ are signal ratios of the lamp to the reference lamp for each polarizer orientation, respectively. $L_{\parallel,\mathrm{ref}}(\lambda, T)$ and $L_{\perp,\mathrm{ref}}(\lambda, T)$ are spectral radiances of the reference lamp for each polarizer orientation, respectively and were calculated by

$$L_{\parallel,\mathrm{ref}}(\lambda) = \frac{1}{2} \cdot R_{\parallel,\mathrm{ref,BB}}(\lambda) \cdot L_{\mathrm{BB}}(\lambda, T) \tag{3-4}$$

$$L_{\perp,\mathrm{ref}}(\lambda) = \frac{1}{2} \cdot R_{\perp,\mathrm{ref,BB}}(\lambda) \cdot L_{\mathrm{BB}}(\lambda, T). \tag{3-5}$$

When a lamp is calibrated by comparing with blackbody, the blackbody temperature was adjusted in order to match the spectroradiometer signals for the blackbody and lamp. Figure 3-2 shows signal ratios of the lamp to the blackbody.

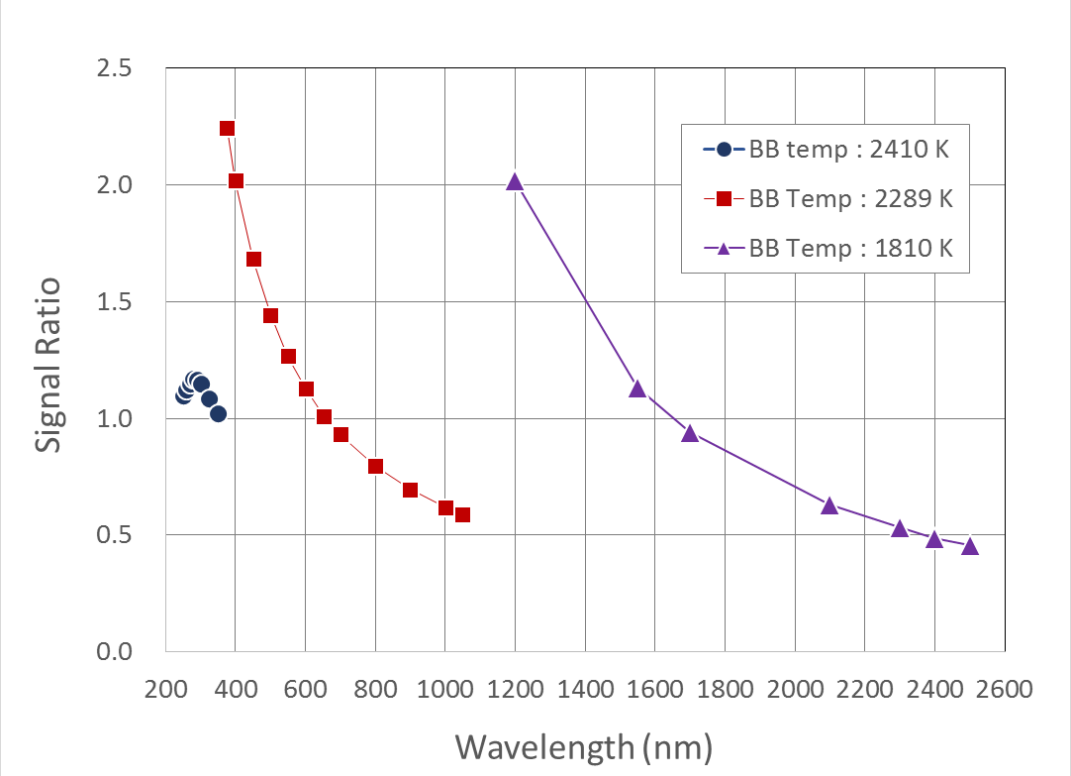

Figure 3-2. Signal ratio between a lamp and blackbody.

Table 3-2 shows average spectral radiances measured at KRISS before and after the measurement of VNIIOFI. Table 3-3 shows average spectral radiances measured at KRISS before and after the measurement of NIM.

Table 3-2. Average spectral radiances measured at KRISS before and after the measurement of VNIIOFI.

	Wavelength (nm)	Lamp 12-04.91 [W/(㎡ sr nm)]	Lamp 22-04.87 [W/(㎡ sr nm)]	Lamp 155-02.86 [W/(㎡ sr nm)]
1	250	5.1429.E-03	5.9961.E-03	5.3498.E-03
2	260	1.0915.E-02	1.2379.E-02	1.1252.E-02
3	270	2.1928.E-02	2.3977.E-02	2.2290.E-02
4	280	4.1127.E-02	4.3457.E-02	4.1379.E-02
5	290	7.2306.E-02	7.4517.E-02	7.2241.E-02
6	300	1.2022.E-01	1.2231.E-01	1.1945.E-01
7	325	3.5454.E-01	3.5722.E-01	3.5023.E-01
8	350	8.5894.E-01	8.6177.E-01	8.4678.E-01
9	375	1.7965.E+00	1.7965.E+00	1.7744.E+00
10	400	3.3490.E+00	3.3362.E+00	3.3154.E+00
11	450	8.9374.E+00	8.8571.E+00	8.8800.E+00
12	500	1.8372.E+01	1.8206.E+01	1.8300.E+01
13	550	3.1432.E+01	3.1228.E+01	3.1378.E+01
14	600	4.7070.E+01	4.6943.E+01	4.7064.E+01
15	656.3	6.6027.E+01	6.6066.E+01	6.6102.E+01
16	700	8.0426.E+01	8.0670.E+01	8.0615.E+01
17	800	1.0850.E+02	1.0922.E+02	1.0900.E+02
18	900	1.2650.E+02	1.2734.E+02	1.2725.E+02
19	1000	1.3415.E+02	1.3492.E+02	1.3521.E+02
20	1050	1.3468.E+02	1.3536.E+02	1.3584.E+02
21	1200	1.2670.E+02	1.2740.E+02	1.2785.E+02
22	1550	8.8954.E+01	8.9235.E+01	8.9976.E+01
23	1700	7.3449.E+01	7.3610.E+01	7.4400.E+01
24	2100	4.2198.E+01	4.2508.E+01	4.2633.E+01
25	2300	3.1579.E+01	3.1919.E+01	3.1931.E+01
26	2400	2.7153.E+01	2.7603.E+01	2.7458.E+01
27	2500	2.3730.E+01	2.4078.E+01	2.3982.E+01

Table 3-3. Average spectral radiances measured at KRISS before and after the measurement of NIM.

	Wavelength (nm)	Lamp 12-04.91 [W/(㎡ sr nm)]	Lamp 22-04.87 [W/(㎡ sr nm)]	Lamp 155-02.86 [W/(㎡ sr nm)]
1	250	4.9982.E-03	5.9561.E-03	5.2492.E-03
2	260	1.0705.E-02	1.2380.E-02	1.1087.E-02
3	270	2.1510.E-02	2.3966.E-02	2.2049.E-02
4	280	4.0541.E-02	4.3551.E-02	4.1016.E-02
5	290	7.1315.E-02	7.4865.E-02	7.1813.E-02
6	300	1.1864.E-01	1.2301.E-01	1.1872.E-01
7	325	3.5112.E-01	3.5990.E-01	3.4867.E-01
8	350	8.5217.E-01	8.6981.E-01	8.4396.E-01
9	375	1.7814.E+00	1.8099.E+00	1.7686.E+00
10	400	3.3212.E+00	3.3616.E+00	3.3027.E+00
11	450	8.8481.E+00	8.9254.E+00	8.8411.E+00
12	500	1.8189.E+01	1.8323.E+01	1.8225.E+01
13	550	3.1163.E+01	3.1409.E+01	3.1265.E+01
14	600	4.6756.E+01	4.7182.E+01	4.6922.E+01
15	656.3	6.5683.E+01	6.6390.E+01	6.5929.E+01
16	700	8.0121.E+01	8.1073.E+01	8.0435.E+01
17	800	1.0820.E+02	1.0976.E+02	1.0877.E+02
18	900	1.2616.E+02	1.2809.E+02	1.2688.E+02
19	1000	1.3354.E+02	1.3578.E+02	1.3468.E+02
20	1050	1.3391.E+02	1.3624.E+02	1.3525.E+02
21	1200	1.2586.E+02	1.2813.E+02	1.2726.E+02
22	1550	8.7942.E+01	8.9656.E+01	8.9429.E+01
23	1700	7.2511.E+01	7.3976.E+01	7.3872.E+01
24	2100	4.1718.E+01	4.2507.E+01	4.2255.E+01
25	2300	3.1433.E+01	3.1879.E+01	3.1751.E+01
26	2400	2.7063.E+01	2.7571.E+01	2.7330.E+01
27	2500	2.3534.E+01	2.4051.E+01	2.3764.E+01

3.5.2. Evaluation of uncertainties

Uncertainty components of spectral radiance of artifacts include the spectral radiance scale realization at KRISS, wavelength accuracy, lamp current, polarizer orientation, lamp alignment, and signal ratio measurement. Uncertainty of the spectral radiance scale realization is shown in the Table 3-1. Spectral radiance uncertainty due to wavelength accuracy was evaluated by using Eq. (3-1) with the wavelength uncertainty of the spectroradiometer. Uncertainties due to other components such as lamp current, polarizer orientation, and lamp alignment were evaluated by experimental measurements [6] for each components at several wavelengths as below.

$$u\big(f(x_1, x_2, \cdots, x_i, \cdots)\big)_{x_i = x_0} = \frac{1}{2} \cdot |\{f(x_1, x_2, \cdots, x_i + u(x_i), \cdots) - f(x_1, x_2, \cdots,\ x_i - u(x_i), \cdots)\}| \tag{3-6}$$

In case of uncertainty evaluation due to lamp alignment, measurements were made for every components related to the alignment such as the translation (x, y, z) and rotation (θ, φ). Table 3-4 shows the uncertainty budget of spectral radiance measurement of artifacts at KRISS.

Table 3-4. Uncertainty budget of spectral radiance measurement of lamps at KRISS.

		Relative standard uncertainty (k=1, %)						
	Wavelength (nm)	Spectral radiance scale realization	Wavelength accuracy	Polarizer orientation	Lamp current	Lamp alignment	Signal ratio measurement	Combined relative Standard uncertainty
1	250	0.65	0.38	0.10	0.07	0.89	0.58	**1.31**
2	260	0.63	0.35	0.10	0.07	0.79	0.28	**1.11**
3	270	0.60	0.32	0.10	0.07	0.70	0.18	**1.00**
4	280	0.58	0.29	0.10	0.07	0.60	0.20	**0.92**
5	290	0.56	0.27	0.10	0.07	0.51	0.14	**0.82**
6	300	0.55	0.25	0.10	0.07	0.41	0.12	**0.75**
7	325	0.50	0.21	0.10	0.06	0.38	0.05	**0.68**
8	350	0.47	0.17	0.10	0.05	0.35	0.03	**0.62**
9	375	0.48	0.16	0.10	0.04	0.32	0.03	**0.61**
10	400	0.45	0.13	0.10	0.04	0.29	0.02	**0.56**
11	450	0.40	0.10	0.10	0.02	0.28	0.02	**0.51**
12	500	0.36	0.08	0.10	0.02	0.26	0.01	**0.47**
13	550	0.33	0.06	0.10	0.02	0.25	0.01	**0.43**
14	600	0.31	0.05	0.10	0.02	0.23	0.01	**0.40**
15	656.3	0.29	0.03	0.10	0.02	0.22	0.01	**0.38**
16	700	0.27	0.03	0.10	0.02	0.22	0.01	**0.36**
17	800	0.24	0.02	0.10	0.02	0.20	0.01	**0.33**
18	900	0.22	0.01	0.10	0.02	0.18	0.01	**0.30**
19	1000	0.20	0.01	0.10	0.02	0.22	0.01	**0.32**
20	1050	0.20	0.01	0.10	0.02	0.24	0.01	**0.32**
21	1200	0.25	0.01	0.10	0.02	0.30	0.01	**0.40**
22	1550	0.21	0.01	0.10	0.02	0.43	0.01	**0.49**
23	1700	0.19	0.01	0.10	0.02	0.48	0.01	**0.53**
24	2100	0.17	0.01	0.10	0.02	0.58	0.01	**0.61**
25	2300	0.16	0.01	0.10	0.02	0.62	0.01	**0.65**
26	2400	0.16	0.01	0.10	0.02	0.65	0.01	**0.67**
27	2500	0.15	0.01	0.10	0.02	0.67	0.01	**0.70**

4. Measurements at NIM

4.1. Description of measurement facility

Spectral radiance scale was realized by using a high-temperature blackbody BB3500M [7,8]. The cylindrical cavity of the BB3500M had the depth of 30 mm, diameter of 59 mm and opening diameter of 15mm. The BB3500M was a windowless blackbody, and the effective emissivity estimated using a Monte-Carlo method calculation was about 0.999 (see the section 5.2 for more details). The temperature of the BB3500M varied

from 1600 K to 2424 K in depends of spectral range to match spectral radiance of a tungsten strip lamp. From 250 nm to 400 nm, the temperature of the blackbody was about 2370 K to 2424 K. From 400 nm to 1100 nm, the temperature of the blackbody was about 2276 K to 2372 K. From 800 nm to 1400 nm, the temperature of the blackbody was about 2010 K. From 1400 nm to 2500 nm, the temperature of the blackbody was about 1600 K to 1726 K.

The comparison lamp was measured by direct comparing with HTBB, and without any other transfer standards. The measurement system of spectral radiance of NIM was listed in Figure 4-1.

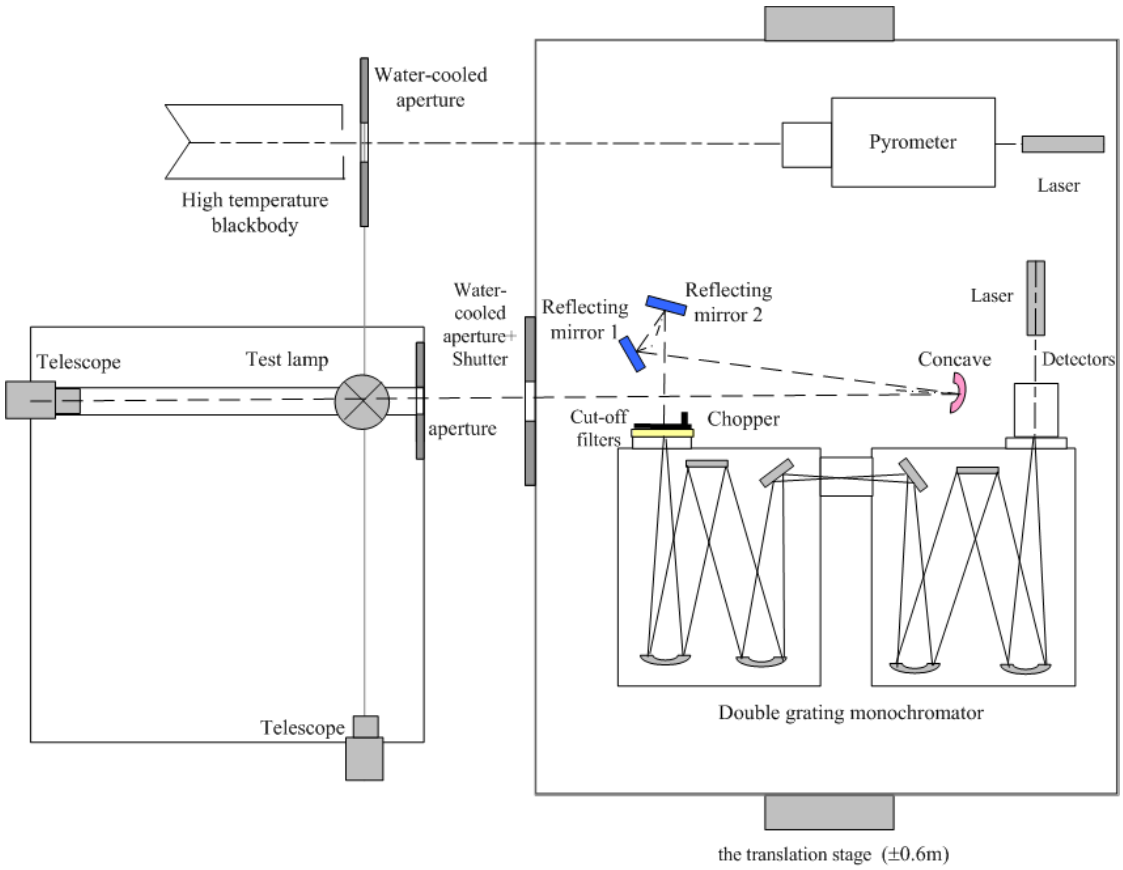

Figure 4-1. Measurement system of spectral radiance.

The imaging optics consisted of a spherical concave mirror and two flat mirrors. The concave mirror had diameter of 110 mm and focal length of 550 mm. The distance from the mirror to the source was 1100 mm. Therefore, the image of the measuring source (strip of the lamp or aperture of the blackbody) was focused on the entrance slit of the monochromator with magnification 1:1. A mask was put in front of the entrance slit of the monochromator to limit the target spot size of the tungsten strip and the water-cooled aperture was 0.6 mm wide by 0.8 mm tall rectangle. The solid angle of spectral radiance measurement is approximately 0.008 sr.

The spectroradiometer of NIM was based on a double-grating monochromator of M207D, made by McPherson, Inc. Three pairs of gratings (1800, 1200 and 600 g/mm) were used to cover the wavelength range from 250 nm to 2500 nm. The focal length of the monochromator was 0.67 m, f/No. is 5.8, and the dispersion is (0.83 ~ 2.48) nm/mm. The spectral bandwidth of the monochromator over the working wavelength range was from 0.50 nm to 1.49 nm. Three detectors were used for the working wavelength range: a R3896 photomultiplier, a Si detector, and a thermo-electrically cooled InGaAs detector with a thermoelectric cooling temperature of -85°C. A 226 Hz chopper and two-phase lock in amplifier were used in infrared wavelength. The chopper was placed in front of the entrance slit of the monochromator, with limiting apertures to cut down stray radiation. A set of second order cut-off filters was mounted in front of the entrance slit.

The HTBB and lamp were compared by using a spectroradiometer based on a double grating monochromator with a set of detectors and imaging optics. The spectroradiometer were set up on the translation stage. The translation of the stage was ±600 mm.

Firstly, the temperature of the blackbody BB3500M was measured by a LP4 pyrometer, the temperature of which was traced to the Pt-C and Re-C fixed point blackbody of the Division of the Thermometry and Material

Evaluation of NIM.

Next, the strip shape of water-cooled aperture in front of the blackbody was imaged on the entrance slit of the double grating monochromator, and then the radiance signal of the blackbody was measured over the specified wavelength range.

Then the translation stage was moved to the lamp position. The strip of the tungsten lamp was imaged on the entrance slit of the double grating monochromator, and the radiance signal of the test lamp was measured over the specified wavelength range.

Finally, the spectral radiance of the test lamp can be calculated according to the signal ratio of the blackbody and the test lamp.

4.2. Spectral radiance scale of NIM

The NIM primary scale for spectral radiance is realized by using a high temperature blackbody source, the temperature of which is measured by using a pyrometer as a comparator traced to the Re-C fixed point blackbody of Division of Thermometry and Materials Evaluation of NIM. The uncertainty of pyrometer is 0.50 K (k = 2) at 2011.05 K and 0.95 K (k = 2) at 2746.97 K, which is traceably to ITS-90. The uncertainty analysis of the blackbody temperature measurement and the spectral radiance scale realization were listed in Table 4-1 and Table 4-2 respectively.

Table 4-1. Uncertainty budget of the blackbody temperature measurement

Wavelength range (nm)	Temperature of HTBB (K)	Uncertainty of Pyrometer (K)	Instability of Pyrometer (K)	Repeatability of measurement including realighment(K)	Uncertainty of temperature measurement of HTBB (K)
250~375	2423	0.5	0.1	0.1	0.5196
400~800	2372	0.5	0.1	0.1	0.5196
900~1200	2010	0.5	0.1	0.1	0.5196
1550~2500	1600	0.5	0.1	0.1	0.5196

Table 4-2. The transfer standard and traceability

No.	Device	Type	Manufactor	Descriptions	Uncertainty	Traceability
1	Pyrometer	LP4;	Germany;	Range: 900℃ ~3000℃	T=1737.90℃ U=0.50℃ (k=2)	Re-C fixed point blackbody of Division of Thermometry and Materials Evaluation of NIM
		RT9032-20#	NIM		T=2473.82℃ U=0.95℃ (k=2)	
2	Digital voltage meter	34420A	Agilent	0.01V~100 V; Accuracy: 0.005%	$U=12\times10^{-6}$ V~6×10^{-6} V (k=2)	the ampere and volt standard of NIM
3	Standard resistance	BZ6	Shanghai Ammeter Factory of China	0.01 class; 0.01Ω,10A	$U=33\times10^{-6}$ Ω (k=3)	the resistance standard of NIM

4.3. Laboratory transfer standards

The electrical measurements of the digital voltmeter 34420A (uncertainty of 0.011%, k=1) and the 0.001 Ω standard resistor (uncertainty of 1.1×10^{-5}, k =1) are traceable to the latest realization of the ampere and volt.

4.4. Laboratory conditions

Temperature range: (20±1) ℃,
Humidity: (55~65) %RH.

4.5. Calibration results of the comparison lamps

Table 4-3 shows the measurement results of comparison lamps. Table 4-4 shows the uncertainty budget of the comparison lamp spectral radiance measurements.

Table 4-3. Measurement results of comparison lamps.

No.		**Lamp 12-04.91**	**Lamp 22-04.87**	**Lamp 155-02.86**
	Wavelength (nm)	Spectral Radiance W/(m^2 sr nm)	Spectral Radiance W/(m^2 sr nm)	Spectral Radiance W/(m^2 sr nm)
1	250	5.2300E-03	6.2630E-03	5.2760E-03
2	260	1.1010E-02	1.2870E-02	1.1140E-02
3	270	2.1830E-02	2.4470E-02	2.2290E-02
4	280	4.0830E-02	4.4160E-02	4.1120E-02
5	290	7.1930E-02	7.6100E-02	7.1800E-02
6	300	1.1990E-01	1.2520E-01	1.1940E-01
7	325	3.5240E-01	3.6480E-01	3.4930E-01
8	350	8.5120E-01	8.7740E-01	8.4230E-01
9	375	1.7680E+00	1.8160E+00	1.7510E+00
10	400	3.3040E+00	3.3710E+00	3.2880E+00
11	450	8.7880E+00	8.8950E+00	8.7400E+00
12	500	1.8030E+01	1.8210E+01	1.7980E+01
13	550	3.0920E+01	3.1250E+01	3.0880E+01
14	600	4.6510E+01	4.7050E+01	4.6480E+01
15	656.3	6.5470E+01	6.6370E+01	6.5520E+01
16	700	7.9940E+01	8.1180E+01	8.0090E+01
17	800	1.0810E+02	1.0990E+02	1.0840E+02
18	900	1.2600E+02	1.2820E+02	1.2650E+02
19	1000	1.3320E+02	1.3580E+02	1.3390E+02
20	1050	1.3350E+02	1.3560E+02	1.3430E+02
21	1200	1.2510E+02	1.2670E+02	1.2690E+02
22	1550	8.6990E+01	8.8090E+01	8.8040E+01
23	1700	7.1680E+01	7.2540E+01	7.2570E+01
24	2100	4.1560E+01	4.2060E+01	4.2130E+01
25	2300	3.1450E+01	3.1920E+01	3.1920E+01
26	2400	2.7130E+01	2.7680E+01	2.7590E+01
27	2500	2.3360E+01	2.4110E+01	2.4200E+01

Table 4-4. Measurement results of comparison lamp spectral radiance measurements

No.		Type A Uncertainty in Value (%)	Type B Uncertainty in Value (%)										RMS total (%)
	Wavelength (nm)	*R* (signal ratio)	Lamp Alignment	Temperature Measurement of HTBB	Non-Uniformity of HTBB	Instability of HTBB	Correction of different Size of Source	Non-linearity of measurement system	Lamp Current	Wavelength	Polarization effect	Bandwidth	u_c
1	**250**	0.520	0.483	0.509	0.057	0.057	0.037	0.100	0.078	0.019	0.200	0.046	**0.910**
2	**260**	0.490	0.310	0.490	0.055	0.055	0.036	0.100	0.075	0.007	0.200	0.044	**0.800**
3	**270**	0.460	0.169	0.472	0.053	0.053	0.035	0.100	0.072	0.008	0.200	0.034	**0.730**
4	**280**	0.360	0.150	0.455	0.051	0.051	0.033	0.100	0.070	0.005	0.200	0.028	**0.650**
5	**290**	0.350	0.120	0.439	0.049	0.049	0.032	0.100	0.067	0.002	0.200	0.023	**0.630**
6	**300**	0.320	0.115	0.424	0.047	0.047	0.031	0.100	0.065	0.003	0.200	0.017	**0.600**
7	**325**	0.185	0.236	0.392	0.044	0.044	0.029	0.100	0.060	0.006	0.200	0.012	**0.550**
8	**350**	0.150	0.161	0.364	0.041	0.041	0.027	0.100	0.056	0.007	0.200	0.008	**0.490**
9	**375**	0.150	0.132	0.340	0.038	0.038	0.025	0.100	0.052	0.005	0.200	0.006	**0.460**
10	**400**	0.150	0.108	0.332	0.037	0.037	0.024	0.100	0.049	0.004	0.200	0.004	**0.450**
11	**450**	0.100	0.125	0.295	0.033	0.033	0.022	0.100	0.043	0.004	0.200	0.002	**0.410**
12	**500**	0.100	0.112	0.266	0.030	0.030	0.019	0.100	0.039	0.003	0.200	0.001	**0.380**
13	**550**	0.100	0.112	0.242	0.027	0.027	0.018	0.100	0.036	0.003	0.200	0.000	**0.370**
14	**600**	0.100	0.112	0.221	0.025	0.025	0.016	0.100	0.033	0.002	0.200	0.000	**0.350**
15	**656.3**	0.100	0.112	0.202	0.023	0.023	0.015	0.100	0.030	0.002	0.200	0.000	**0.340**
16	**700**	0.100	0.112	0.190	0.021	0.021	0.014	0.100	0.028	0.002	0.200	0.000	**0.330**
17	**800**	0.150	0.039	0.166	0.019	0.019	0.012	0.100	0.024	0.005	0.200	0.000	**0.320**
18	**900**	0.150	0.069	0.114	0.023	0.023	0.015	0.100	0.022	0.012	0.200	0.000	**0.300**
19	**1000**	0.150	0.090	0.102	0.021	0.021	0.014	0.100	0.020	0.010	0.200	0.000	**0.300**
20	**1050**	0.150	0.099	0.097	0.020	0.020	0.013	0.100	0.019	0.010	0.200	0.000	**0.310**
21	**1200**	0.150	0.132	0.085	0.017	0.017	0.011	0.100	0.016	0.008	0.200	0.000	**0.310**
22	**1550**	0.200	0.150	0.104	0.021	0.021	0.014	0.100	0.013	0.009	0.200	0.000	**0.350**
23	**1700**	0.250	0.166	0.095	0.019	0.019	0.013	0.100	0.011	0.008	0.200	0.000	**0.390**
24	**2100**	0.300	0.180	0.077	0.016	0.016	0.010	0.100	0.009	0.006	0.200	0.000	**0.420**
25	**2300**	0.400	0.206	0.070	0.014	0.014	0.009	0.100	0.008	0.005	0.200	0.000	**0.510**
26	**2400**	0.450	0.218	0.067	0.014	0.014	0.009	0.100	0.008	0.005	0.200	0.000	**0.550**
27	**2500**	0.500	0.332	0.065	0.013	0.013	0.009	0.100	0.008	0.005	0.200	0.000	**0.640**

5. Measurements at VNIIOFI

5.1. Description of measurement facility

A diagram of the spectral radiance measurement facility is shown in Fig.5-1. The facility is based on a high-temperature blackbody BB3500M manufactured by VNIIOFI [9]. The blackbody (1 in the diagram) and lamps (2) to be calibrated are located next to each other on an optical table. In front of the table there is a translation stage (10), which can moves parallel to the table, with a spectral comparator. The comparator consists of double grating monochromator (4), a set of detectors (5), focusing toroidal mirror (8) and a flat mirror (7). In front of the entrance slit of the monochromator there is a polarizer (6). The pyrometer (3) of the TSP type [10] was used for measuring temperature of the blackbody. In front of each radiation source (lamps and the blackbody) there is a shutter.

The diameter of the focusing mirror was 120 mm, and the distance to the source (lamp or blackbody) was 1200 mm. The distance to the monochromator was also 1200 mm. Therefore, magnification of the optics was 1. The entrance slit of the monochromator was rectangular with 0.6 mm width and 0.8 mm height.

The monochromator was of the DTMc300 type manufactured by Bentham Instruments Ltd (UK). It had three pairs of gratings:

- 1200 g/mm for the spectral range from 200 nm to 400 nm,
- 1200 g/mm for the spectral range from 400 nm to 1100 nm and
- 600 g/mm for the spectral range from 1100 nm to 2500 nm.

The bandwidth during the comparison measurements was approximately:

- 2.4 mm in the spectral range from 250 nm to 1100 nm and
- 4.8 mm in the spectral range from 1100 nm to 2500 nm.

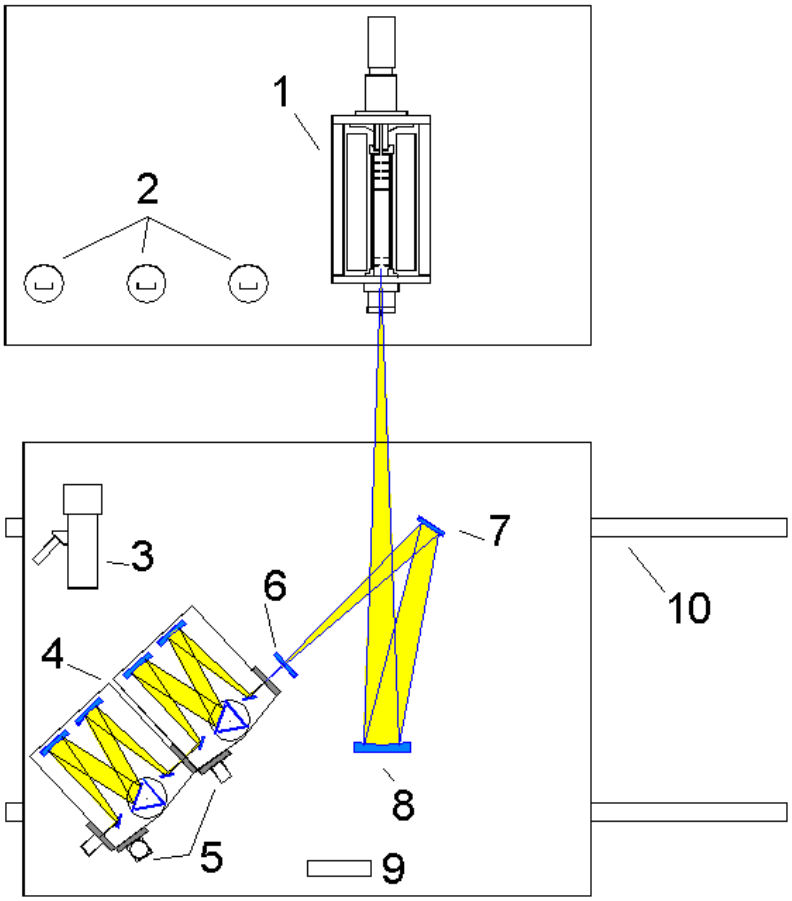

Figure 5-1. VNIIOFI spectral radiance measurement facility. 1 – high-temperature blackbody, 2 – strip lamps, 3 – pyrometer, 4 – monochromator, 5 – detectors, 6 – polarizer, 7 – flat mirror, 8 – focusing mirror, 9 – alignment laser, 10 – translation stage.

The following photo-detectors were used:

- PMT in the spectral range from 250 nm to 400 nm,
- Si photodiode in the spectral range from 400 nm to 1050 nm,
- InGaAs photodiode in the spectral range from 1000 nm to 1700 nm and
- Extended InGaAs photodiode in the spectral range from 1700 nm to 2500 nm

All detectors were manufactured by Hamamatsu Photonics. The detectors were installed directly on the exit slits.

Alignments of the lamps and blackbody was performed using a laser (9), which was connected to the exit slit instead of one of the detectors.

The procedure of the measurement was the following:

- polarizer was set to the orientation 1,
- monochromator was set to the wavelength λ,
- spectral comparator was moved to the Standard source (the blackbody when a VNIIOFI standard lamp was calibrated, or a VNIIOFI standard lamp when the comparison lamps were calibrated),
- detector signal $i_{1,SS}(\lambda)$ was measured,
- shutter closed and the dark signal measured,
- spectral comparator was moved to the calibrated lamp,
- detector signal $i_{1,Lamp}(\lambda)$ was measured,
- shutter closed and the dark signal measured,
- then the monochromator was set to the next wavelength and all measurements were repeated for each wavelength in a spectral sub-range. The sub-range depends on a detector and a polarizer.
- then the polarizer was set to the orientation 2, and all measurements were repeated for each wavelength in the same spectral sub-range: signals $i_{2,SS}(\lambda)$ and $i_{2,Lamp}(\lambda)$ were measured,
- the measurements were carried out in all spectral sub-ranges to cover the range 250 nm to 2500 nm.

Spectral radiance of the calibrated lamp was calculated as

$$L_{\lambda,\mathrm{Lamp}}(\lambda)=\frac{1}{2}\left(\frac{i_{1,\mathrm{Lamp}}(\lambda)}{i_{1,\mathrm{SS}}(\lambda)}+\frac{i_{2,\mathrm{Lamp}}(\lambda)}{i_{2,\mathrm{SS}}(\lambda)}\right)\cdot L_{\lambda,\mathrm{SS}}(\lambda) \tag{5-1}$$

where $L_{\lambda,\mathrm{SS}}(\lambda)$ is spectral radiance of the standard source.

5.2. Spectral radiance scale of VNIIOFI

The primary scale was realized with the blackbody and transfer to a group of three VNIIOFI standard lamps. Each standard lamp was measured against the blackbody three times with independent alignment. Spectral Radiance assigned to each standard lamp was an average of three independent measurements:

$$L^{m}_{\lambda,\mathrm{SLamp}}(\lambda)=\frac{1}{3}\sum_{j=1}^{3}L^{m,j}_{\lambda,\mathrm{SLamp}}(\lambda)=\frac{1}{3}\sum_{j=1}^{3}\left[\frac{1}{2}\left(\frac{i_{1,\mathrm{Lamp}}(\lambda)}{i_{1,\mathrm{SS}}(\lambda)}+\frac{i_{2,\mathrm{Lamp}}(\lambda)}{i_{2,\mathrm{SS}}(\lambda)}\right)\cdot L_{\lambda,\mathrm{BB}}(\lambda,T)\right]^{j} \tag{5-2}$$

where *m* indicates a lamp number and *j* indicates an independent measurement. Spectral radiance of the blackbody was calculated with the Planck equation:

$$L_{\lambda,\mathrm{BB}}(\lambda,T)=\varepsilon_{eff}\,\frac{c_1}{\pi\cdot n^2\lambda^5}\left(\exp\frac{c_2}{n\lambda T}-1\right)^{-1} \tag{5-3}$$

where c_1 and c_2 – the first and second radiation constants, λ is wavelength in air, T – temperature of the blackbody, n – air refractive index and $\varepsilon_{\mathrm{eff}}$ – effective emissivity of the blackbody.
c_1= $3.741772\cdot10^{-16}$ W m^2 and c_2=$1.438777\cdot10^{-2}$ K m with uncertainties negligible comparing to other uncertainty components.

Refractive index *n* was calculated according to the Ref [11] and approximately equals to 1.00028 **with standard uncertainty** estimated as **0.00002.**

Emissivity $\varepsilon_{\mathrm{eff}}$ was estimated as 0.9995 **with standard uncertainty of 0.0003** in visible and IR, and increasing up **to 0.001** in UV. The special software STEEP for blackbody non-isothermal cavity emissivity calculation was used. The software is based on the Monte-Carlo method and allows calculating spectral emissivities for any axis-symmetrical cavity shapes, any temperature distribution along the cavity and any combination of specular – diffuse reflection future of the cavity walls [12, 13]. The BB3500M emissivity and its uncertainty were estimated assuming the spectrally independent reflectance of the graphite cavity walls of 0.85±0.05 with diffusely varies from 0.8 to 1 and applying different temperature profiles along the side walls and the cavity bottom. The temperature profiles were modeled based on experimental measurements of the radiation temperature distribution. More details of applying the STEEP software for emissivity estimation are given in [14]. Since the temperature gradient has a stronger effect on the blackbody radiation in the UV, the uncertainty of emissivity in UV is higher than in visible and IR. However, if the temperature profile is known too rough, the emissivity can be decrease down to 0.999 with the same uncertainty 0.001 in the whole spectrum range. The experiments approaches of measurements of the pyrographite high-temperature blackbody emissivity [14, 15, 16] well agreed with its estimation between 0.9990 and 1.0000.

The temperature of the blackbody was measured with a radiance pyrometer calibrated against the high-temperature fixed points (HTFP) Co-C (1597.4 K), Pt-C (2011.4 K) and Re-C (2747.8 K). Thermodynamic temperatures of the HTFPs were measured by means of primary radiometric methods within the international project “Implementing the new Kelvin (InK)” [17]. The overall **standard uncertainty of temperature** measurement was **0.4 K** including effects related to the pyrometer (stability and SSE) and to the HTFP realization.

Table 5-1 presented the uncertainty budget of the primary scale including the uncertainty components associated with the blackbody, standard lamps and spectral comparator. Other uncertainty components, associated with the blackbody, lamp and spectral comparator are:

Blackbody uniformity: The pyrometer and the spectral comparator see difference arrears on the blackbody

cavity bottom. Therefore, due to non-uniformity of the cavity the pyrometer and the comparator receive radiation with different affective temperature. We estimate the associated **standard uncertainty** as **0.3 K** in terms of temperature.

Blackbody stability: The maximum drift of the blackbody temperature between two sequence measurements was 0.2 K. The associated uncertainty was evaluated as $0.2/2/3^{1/2}$ = **0.06 K**.

Lamp current was measured with standard uncertainty of **1.5 mA**. The corresponding uncertainty in terms of spectral radiance at 656 nm was determined experimentally and re-calculated for other wavelength using the Planck equation.

Wavelength setting **uncertainty** of **0.2 nm** below 1050 nm and 0.4 above 1050 nm was re-calculated into radiance uncertainty using the data of Lamp/BB ratio spectral dependence.

During measurements we observed **Discrepancy** when **changed detectors, polarizers gratings and filters**. We don't know the exact reason of this discrepancy; it could be spatial non-uniformity of detectors, non-perfectness of polarizers and filters and scattering light. Associated uncertainty was estimated on the base on observed discrepancy.

The **Lamp/BB Ration uncertainty** was based on **combined** typical **standard deviation of** detectors **signals** corresponding to the lamp, blackbody and dark measurements. This uncertainty is correlated with the uncertainty component evaluated as standard deviation of three independent measurements (the last column of the Table 5-1). Therefore, the lamp/BB ratio uncertainty was reduced by the factor of $\sqrt{n}$, where n=3 – the number of the independent measurements.

Table 5-1. Uncertainty budget of the primary scale (including transfer to the standard lamps)

No.	Wavelength, nm	Relative standard uncertainty, % (in terms of spectral radiance)										
		Refractive index of air	Blackbody emissivity	Blackbody temperature (0.4 K)	Blackbody uniformity (0.3 K)	Blackbody stability (0.1 K)	Lamp current (1.5 mA)	Wavelength (0.2 nm)	Discrepancy between detectors, filters, polarizer	Lamp/BB Ratio Standard Deviation	Lamp reproducibility (Stan.Dev. between independent measurements)	**Combined standard uncertainty**
		B	B	B	B	B	B	B	B	A	A	
1	250	0.05	0.10	0.45	0.33	0.07	0.09	0.02	0.20	0.55	0.60	**1.02**
2	260	0.04	0.09	0.43	0.32	0.06	0.09	0.02	0.20	0.40	0.55	**0.90**
3	270	0.04	0.08	0.41	0.31	0.06	0.08	0.03	0.20	0.30	0.50	**0.82**
4	280	0.04	0.07	0.40	0.30	0.06	0.08	0.07	0.20	0.25	0.48	**0.78**
5	290	0.04	0.06	0.38	0.29	0.06	0.08	0.09	0.20	0.22	0.45	**0.74**
6	300	0.04	0.05	0.37	0.28	0.06	0.07	0.10	0.20	0.20	0.42	**0.70**
7	325	0.03	0.05	0.34	0.26	0.05	0.07	0.10	0.15	0.20	0.36	**0.63**
8	350	0.03	0.04	0.32	0.24	0.05	0.06	0.10	0.15	0.20	0.30	**0.56**
9	375	0.03	0.04	0.30	0.22	0.04	0.06	0.10	0.15	0.15	0.28	**0.52**
10	400	0.03	0.03	0.28	0.21	0.04	0.06	0.09	0.15	0.10	0.25	**0.47**
11	450	0.02	0.03	0.25	0.19	0.04	0.05	0.07	0.15	0.05	0.22	**0.41**
12	500	0.02	0.03	0.22	0.17	0.03	0.04	0.06	0.10	0.03	0.20	**0.36**
13	550	0.02	0.03	0.20	0.15	0.03	0.04	0.05	0.10	0.03	0.18	**0.33**
14	600	0.02	0.03	0.19	0.14	0.03	0.04	0.04	0.10	0.03	0.17	**0.30**
15	656.3	0.02	0.03	0.17	0.13	0.03	0.03	0.04	0.10	0.03	0.16	**0.28**
16	700	0.01	0.03	0.16	0.12	0.02	0.03	0.04	0.10	0.02	0.15	**0.26**
17	800	0.01	0.03	0.14	0.10	0.02	0.03	0.03	0.10	0.02	0.15	**0.24**
18	900	0.01	0.03	0.12	0.09	0.02	0.02	0.03	0.10	0.02	0.15	**0.23**
19	1000	0.01	0.03	0.11	0.08	0.02	0.02	0.03	0.10	0.02	0.15	**0.22**
20	1050	0.01	0.03	0.11	0.08	0.02	0.02	0.04	0.10	0.02	0.15	**0.22**
21	1200	0.01	0.03	0.09	0.07	0.01	0.02	0.04	0.10	0.02	0.15	**0.22**
22	1550	0.00	0.03	0.08	0.05	0.01	0.02	0.04	0.15	0.02	0.15	**0.24**
23	1700	0.00	0.03	0.07	0.05	0.01	0.01	0.03	0.30	0.02	0.20	**0.37**
24	2100	0.00	0.03	0.06	0.04	0.01	0.01	0.02	0.30	0.02	0.30	**0.43**
25	2300	0.00	0.03	0.05	0.04	0.01	0.01	0.02	0.30	0.02	0.35	**0.47**
26	2400	0.00	0.03	0.05	0.04	0.01	0.01	0.02	0.30	0.02	0.40	**0.51**
27	2500	0.00	0.03	0.05	0.04	0.01	0.01	0.02	0.30	0.02	0.48	**0.57**

5.3. Laboratory transfer standards

Three VNIIOFI standard lamps were used to calibrate the comparison lamps. The type of the VNIIOFI

standard lamps was the same as that of the comparison lamps: TRU 1100-2350. Spectral Radiance of the VNIIOFI standard lamps was measured by means of comparing with a high-temperature blackbody; and the APMP.PR-S6 comparison lamps were calibrated against the VNIIOFI standard lamps.

5.4. Laboratory conditions

The laboratory conditions during the comparison lamps measurement were the following:

- Temperature: (23 ± 1) °C;
- Pressure: (98.2 – 98.7) kPa
- Humidity: (70 ± 5) %.

5.5. Calibration results of the comparison lamps

The comparison lamps were measured using the same facility (Fig.5-1). But the blackbody was not used in this stage. The comparison lamps were measured by comparing with three VNIIOFI standard lamps. Each comparison lamp was measure three times; each time by comparing with another standard lamp. Therefore, each comparison lamp was compared with each of the standard lamps.

Table 5-2 shows the measurement results of the comparison lamps. Table 5-3 shows the uncertainty budget of the comparison lamp spectral radiance measurements.

Table 5-2. Measurement results of the comparison lamps

No.		Lamp 12-04.91	Lamp 22-04.87	Lamp 155-02.86
	Wavelength (nm)	Spectral Radiance W/(m^2 sr nm)	Spectral Radiance W/(m^2 sr nm)	Spectral Radiance W/(m^2 sr nm)
1	250	5.1296E-03	6.0782E-03	5.3275E-03
2	260	1.0998E-02	1.2647E-02	1.1262E-02
3	270	2.2055E-02	2.4389E-02	2.2316E-02
4	280	4.1471E-02	4.4337E-02	4.1596E-02
5	290	7.2946E-02	7.6106E-02	7.2680E-02
6	300	1.2105E-01	1.2466E-01	1.2011E-01
7	325	3.5753E-01	3.6377E-01	3.5304E-01
8	350	8.6448E-01	8.7511E-01	8.5305E-01
9	375	1.8072E+00	1.8224E+00	1.7863E+00
10	400	3.3660E+00	3.3769E+00	3.3334E+00
11	450	8.9519E+00	8.9468E+00	8.8748E+00
12	500	1.8318E+01	1.8303E+01	1.8212E+01
13	550	3.1361E+01	3.1395E+01	3.1248E+01
14	600	4.7038E+01	4.7212E+01	4.6966E+01
15	656.3	6.6166E+01	6.6591E+01	6.6193E+01
16	700	8.0758E+01	8.1414E+01	8.0892E+01
17	800	1.0925E+02	1.1038E+02	1.0966E+02
18	900	1.2726E+02	1.2868E+02	1.2793E+02
19	1000	1.3422E+02	1.3569E+02	1.3510E+02
20	1050	1.3434E+02	1.3575E+02	1.3531E+02
21	1200	1.2620E+02	1.2732E+02	1.2721E+02
22	1550	8.7874E+01	8.8433E+01	8.8677E+01
23	1700	7.2254E+01	7.2633E+01	7.3021E+01
24	2100	4.1611E+01	4.1868E+01	4.2108E+01
25	2300	3.1497E+01	3.1815E+01	3.1878E+01
26	2400	2.7170E+01	2.7591E+01	2.7519E+01
27	2500	2.3500E+01	2.3937E+01	2.3802E+01

Table 5-3. Uncertainty budget of the comparison lamps spectral radiance

No.	Wavelength, nm	Relative standard uncertainty, %									
		Scale (Standard lamps)	Stability of Standard lamps	Current Stan. Lamp	Current Com. Lamp	Wavelength (0.2 nm)	Discrepancy between detectors, filters, polarizer)	Lamp/BB Ratio Standard Deviation	Lamp reproducibility (Stan.Dev. between independent measurements	**Combined standard uncertainty**	**Expanded uncertainty (k =2)**
		B	B	B	B	B	B	A	A		
1	250	1.02	0.24	0.09	0.09	0.07	0.20	0.45	0.45	**1.25**	**2.50**
2	260	0.90	0.24	0.09	0.09	0.06	0.20	0.26	0.45	**1.09**	**2.19**
3	270	0.82	0.23	0.08	0.08	0.05	0.20	0.20	0.45	**1.01**	**2.02**
4	280	0.78	0.22	0.08	0.08	0.04	0.20	0.16	0.40	**0.94**	**1.89**
5	290	0.74	0.22	0.08	0.08	0.03	0.20	0.12	0.40	**0.91**	**1.81**
6	300	0.70	0.21	0.07	0.07	0.02	0.20	0.12	0.40	**0.87**	**1.75**
7	325	0.63	0.20	0.07	0.07	0.01	0.10	0.12	0.27	**0.74**	**1.47**
8	350	0.56	0.19	0.06	0.06	0.01	0.50	0.12	0.25	**0.83**	**1.66**
9	375	0.52	0.18	0.06	0.06	0.01	0.05	0.10	0.25	**0.62**	**1.24**
10	400	0.47	0.17	0.06	0.06	0.01	0.04	0.10	0.25	**0.57**	**1.15**
11	450	0.41	0.16	0.05	0.05	0.01	0.04	0.03	0.15	**0.47**	**0.94**
12	500	0.36	0.15	0.04	0.04	0.01	0.03	0.02	0.15	**0.42**	**0.84**
13	550	0.33	0.14	0.04	0.04	0.00	0.03	0.02	0.15	**0.39**	**0.78**
14	600	0.30	0.14	0.04	0.04	0.00	0.03	0.02	0.15	**0.37**	**0.74**
15	656.3	0.28	0.13	0.03	0.03	0.00	0.02	0.02	0.15	**0.35**	**0.70**
16	700	0.26	0.13	0.03	0.03	0.00	0.02	0.02	0.15	**0.33**	**0.66**
17	800	0.24	0.12	0.03	0.03	0.00	0.01	0.02	0.15	**0.31**	**0.63**
18	900	0.23	0.12	0.02	0.02	0.00	0.01	0.02	0.15	**0.30**	**0.60**
19	1000	0.22	0.11	0.02	0.02	0.00	0.01	0.02	0.15	**0.29**	**0.58**
20	1050	0.22	0.11	0.02	0.02	0.00	0.01	0.02	0.18	**0.30**	**0.61**
21	1200	0.22	0.11	0.02	0.02	0.00	0.01	0.02	0.25	**0.35**	**0.71**
22	1550	0.24	0.11	0.02	0.02	0.00	0.10	0.02	0.42	**0.51**	**1.01**
23	1700	0.37	0.11	0.01	0.01	0.00	0.15	0.02	0.50	**0.65**	**1.30**
24	2100	0.43	0.10	0.01	0.01	0.00	0.30	0.02	0.50	**0.73**	**1.47**
25	2300	0.47	0.10	0.01	0.01	0.00	0.30	0.02	0.50	**0.75**	**1.51**
26	2400	0.51	0.10	0.01	0.01	0.00	0.30	0.02	0.50	**0.78**	**1.56**
27	2500	0.57	0.10	0.01	0.01	0.00	0.30	0.02	0.50	**0.82**	**1.65**

The last uncertainty component is a **lamp reproducibility** estimated as a **standard deviation of** results of three **independent measurements.** It includes the uncertainty related to the lamp alignment. Therefore the latter is not presented separately. Because of the small number of independent measurements we prefer the estimate the reproducibility uncertainty as a standard deviation but not standard deviation of the mean, i.e. it was not divided by $\sqrt{3}$.

6. Analysis of measurement results

Three tungsten strip lamps were used as comparison artifacts. The measurement sequence was KRISS → VNIIOFI → KRISS → NIM → KRISS. KRISS collected measurement results and analyzed to calculate differences from the RV and their uncertainties of participants.

Differences from the RV and their uncertainties were calculated by using spectral radiance ratios of participants to the pilot laboratory as below. The details of this analysis method (Ratio Method) are described in Appendix A of this report.

The following notations were used in the analysis.

N Number of participants, including the pilot.

$L_{i,j}$ Spectral radiance of a lamp j (=1 to 3) of a participant i measured by the participant.

$u_{rel}(L_{i,j})$ Relative uncertainty of $L_{i,j}$ reported by the participant i.

$L_{i,j}^{\mathrm{P}}$ Spectral radiance of lamp j of a participant i measured by the pilot.

$u_{rel}(L_{i,j}^{\mathrm{P}})$ Relative uncertainty of the pilot measurement, $L_{i,j}^{\mathrm{P}}$.

L_{ref} Reference spectral radiance of the virtual artifact.

$r_{i,j}$ Spectral radiance ratio between a participant i and the pilot for each artifact.

$u_{\mathrm{rel}}(r_{i,j})$ Relative uncertainty of the spectral radiance ratios.

1) The spectral radiance ratio between a participant *i* and the pilot P for each artifact was calculated by.

$$r_{i,j} = \frac{L_{i,j}}{L_{i,j}^{\mathrm{P}}} \tag{6-1}$$

2) The relative uncertainty of the ratios spectral radiance ratio between a participant *i* and the pilot *p* was calculated by.

$$u_{\mathrm{rel}}(r_{i,j}) = \sqrt{u_{\mathrm{rel}}^2(L_{i,j}) + u_{\mathrm{rel}}^2(L_{i,j}^{\mathrm{P}}) + u_{\mathrm{rel,add}}^2(L_{i,j})}\ , \tag{6-2}$$

where $u_{\mathrm{rel,add}}(L_{i,j})$ is an additional uncertainty in the comparison of lamp *j* of the participant *i* as defined in Ref [1]. In this comparison, no additional uncertainty was introduced, $u_{\mathrm{rel,add}}(L_{i,j}) = 0$.

3) The mean spectral radiance ratio of each participant *i* was calculated by

$$r_i = \left(\prod_{j=1}^{3} r_{i,j}\right)^{1/3}. \tag{6-3}$$

4) The relative uncertainty of the mean spectral radiance ratio of each participant *i* was calculated by.

$$u_{\mathrm{rel}}(r_i) = \sqrt{u_{\mathrm{rel}}^2(\bar{L}_\iota) + u_{\mathrm{rel}}^2(\overline{L_i^{\mathrm{P}}}) + u_{\mathrm{rel,add}}^2(\bar{L}_\iota)}\ , \tag{6-4}$$

where $u_{\mathrm{rel,add}}(\bar{L}_\iota)$ is an average additional uncertainty in the comparison of lamp *j* of the participant *i*. Average uncertainties in Eq. (6-4) can be given by arithmetic mean values when average spectral radiances were calculated by a geometric mean.

Table 6-1 shows the mean spectral radiance ratios and their uncertainties. Averaged spectral radiances measured before and after measurements of VNIIOFI or NIM were used for the calculation of the spectral radiance ratio of each participant, respectively.

Table 6-1. Mean spectral radiance ratios to the pilot and their relative standard uncertainties (*k*=1).

Wavelength nm	KRISS (pilot)		NIM		VNIIOFI	
	Mean spectral radiance ratio	relative uncetainty (%)	Mean spectral radiance ratio	relative uncetainty (%)	Mean spectral radiance ratio	relative uncetainty (%)
250	1	0	1.0341	1.59	1.0023	1.81
260	1	0	1.0242	1.37	1.0100	1.56
270	1	0	1.0156	1.24	1.0080	1.42
280	1	0	1.0079	1.12	1.0113	1.32
290	1	0	1.0083	1.04	1.0121	1.22
300	1	0	1.0114	0.96	1.0105	1.15
325	1	0	1.0063	0.87	1.0116	1.00
350	1	0	1.0019	0.79	1.0098	1.04
375	1	0	0.9953	0.76	1.0090	0.87
400	1	0	0.9977	0.72	1.0076	0.80
450	1	0	0.9928	0.65	1.0037	0.69
500	1	0	0.9905	0.60	0.9992	0.63
550	1	0	0.9916	0.57	0.9996	0.58
600	1	0	0.9942	0.53	1.0010	0.55
656.3	1	0	0.9967	0.51	1.0038	0.51
700	1	0	0.9983	0.49	1.0056	0.49
800	1	0	0.9990	0.46	1.0079	0.45
900	1	0	0.9989	0.43	1.0073	0.43
1000	1	0	0.9973	0.44	1.0018	0.43
1050	1	0	0.9951	0.45	0.9988	0.45
1200	1	0	0.9933	0.51	0.9968	0.54
1550	1	0	0.9854	0.60	0.9881	0.70
1700	1	0	0.9838	0.66	0.9840	0.84
2100	1	0	0.9942	0.74	0.9862	0.95
2300	1	0	1.0024	0.83	0.9975	1.00
2400	1	0	1.0053	0.87	1.0008	1.03
2500	1	0	1.0044	0.95	0.9923	1.08

5) The relative uncertainty of spectral radiance of each participant was adjusted to calculate the weights with cut-off as below.

$$u_{\mathrm{rel,adj}}(\overline{L_i}) = u_{\mathrm{rel}}(\overline{L_i}) \text{ for } u_{\mathrm{rel}}(\overline{L_i}) \geq u_{\mathrm{cut-off}}$$

$$u_{\mathrm{rel,adj}}(\overline{L_i}) = u_{\mathrm{cut-off}} \text{ for } u_{\mathrm{rel}}(\overline{L_i}) < u_{\mathrm{cut-off}}$$

$$u_{\mathrm{cut-off}} = \mathrm{Average}\{u_{\mathrm{rel}}(\overline{L_i})\} \text{ for } u_{\mathrm{rel}}(\overline{L_i}) \leq \mathrm{Median}\{u_{\mathrm{rel}}(\overline{L_i})\}, i = 1,2,3 \quad (6\text{-}5)$$

6) The weight of each participant is given by

$$w_i = u_{\mathrm{rel,adj}}^{-2}(r_i) / \sum_{i=1}^{N} u_{\mathrm{rel,adj}}^{-2}(r_i) \ . \quad (6\text{-}6)$$

7) RV ratio, $r_{\mathrm{RV}} = L_{\mathrm{ref}}/L^{\mathrm{P}}$ is defined as the ratio of reference value (RV) of spectral radiance to the pilot measurement is given by

$$r_{\mathrm{RV}} = \prod_{i=1}^{N} r_i^{w_i} \ . \quad (6\text{-}7)$$

with a constraint of

$$\prod_{i=1}^{N} \left(\frac{L_i}{L_{\mathrm{ref}}}\right)^{w_i} = 1. \quad (6\text{-}8)$$

8) Uncertainty of RV ratio is given by

$$u_{\mathrm{rel}}(r_{\mathrm{RV}}) = \sqrt{\sum_{i=1}^{N} w_i^2 u_{\mathrm{rel}}^2(\overline{L_i}) + (1 - 2w_{\mathrm{P}}) u_{\mathrm{rel}}^2(\overline{L^{\mathrm{P}}})} \ . \quad (6\text{-}9)$$

Table 6-2 shows the cut-off uncertainty, weights of participants, RV ratio, and relative uncertainty of RV ratio.

Table 6-2. Cut-off uncertainty, weights, RV ratio, and relative standard uncertainty of RV ratio.

Wavelength (nm)	Cut-off uncertainty (%)	Weight			RV ratio	Relative standard uncertainty of RV ratio *(k*=1) (%)
		KRISS	NIM	VNIIOFI		
250	1.08	0.3094	0.3676	0.3230	1.0132	1.04
260	0.95	0.3149	0.3651	0.3200	1.0120	0.89
270	0.86	0.3189	0.3648	0.3163	1.0082	0.80
280	0.78	0.3198	0.3697	0.3104	1.0064	0.73
290	0.73	0.3298	0.3711	0.2991	1.0067	0.66
300	0.67	0.3395	0.3743	0.2861	1.0072	0.60
325	0.61	0.3319	0.3645	0.3036	1.0058	0.54
350	0.56	0.3530	0.3925	0.2545	1.0032	0.49
375	0.53	0.3215	0.3627	0.3158	1.0011	0.49
400	0.51	0.3245	0.3583	0.3172	1.0016	0.45
450	0.44	0.3109	0.3549	0.3342	0.9987	0.41
500	0.40	0.3078	0.3539	0.3384	0.9964	0.38
550	0.38	0.3103	0.3492	0.3405	0.9969	0.35
600	0.36	0.3128	0.3479	0.3393	0.9983	0.33
656.3	0.34	0.3145	0.3444	0.3410	1.0002	0.31
700	0.33	0.3154	0.3429	0.3417	1.0013	0.29
800	0.32	0.3263	0.3353	0.3384	1.0023	0.27
900	0.30	0.3317	0.3340	0.3343	1.0021	0.25
1000	0.30	0.3209	0.3370	0.3421	0.9997	0.26
1050	0.31	0.3224	0.3374	0.3402	0.9979	0.26
1200	0.33	0.3009	0.3590	0.3401	0.9965	0.33
1550	0.42	0.3213	0.3697	0.3090	0.9909	0.39
1700	0.46	0.3397	0.3881	0.2722	0.9893	0.42
2100	0.52	0.3349	0.3911	0.2740	0.9940	0.48
2300	0.58	0.3367	0.3754	0.2879	1.0002	0.52
2400	0.61	0.3388	0.3713	0.2899	1.0022	0.54
2500	0.67	0.3480	0.3621	0.2899	0.9994	0.56

9) The Chi-square value χ^2_{obs} for consistency check was calculated by

$$\chi^2_{\text{obs}} = \sum_{i=1}^{3} \frac{(r_i - r_{\text{RV}})^2}{u^2_{\text{rel,adj}}(r_i) \cdot r_i^2} \ , \tag{6-10}$$

and $\chi^2_{\text{obs}} < \chi^2_{0.05}(\nu = 2)$ was obtained. It showed that consistency was satisfied.

10) Difference from the RV of a participant *i* is given by

$$D_i = \frac{r_i}{r_{\text{RV}}} - 1, \tag{6-11}$$

since the difference from the RV is defined as

$$D_i = \frac{L_i}{L_{\text{ref}}} - 1. \tag{6-12}$$

11) The expanded uncertainty of the difference from the RV of participant *i* is given by

$$\mathrm{U}(D_i) = k \cdot (1 + D_i) \cdot \sqrt{u^2_{\text{rel}}(r_{\text{RV}}) - (1 - 2w_{\text{P}}) u^2_{\text{rel}}\left(\overline{L^{\text{P}}}\right) + \ (1 - 2w_i) u^2_{\text{rel}}(\overline{L_i})} \ ; k{=}2 \tag{6-13}$$

Table 6-3 shows the difference from the RV and its uncertainty of each participant.

Table 6-3. Difference from the RV and its expanded uncertainty (*k*=2) of each participant**.**

Wavelength (nm)	KRISS		NIM		VNIIOFI	
	D (%)	*U*(*D*), *k*=2 (%)	*D* (%)	*U*(*D*), *k*=2 (%)	*D* (%)	*U*(*D*), *k*=2 (%)
250	-1.30	2.06	2.07	1.66	-1.07	1.97
260	-1.18	1.76	1.20	1.44	-0.19	1.74
270	-0.81	1.58	0.73	1.30	-0.02	1.61
280	-0.64	1.45	0.15	1.17	0.48	1.51
290	-0.66	1.31	0.16	1.11	0.54	1.47
300	-0.72	1.18	0.41	1.04	0.32	1.42
325	-0.58	1.08	0.05	0.94	0.57	1.20
350	-0.32	0.98	-0.13	0.85	0.65	1.38
375	-0.11	0.97	-0.58	0.80	0.79	1.00
400	-0.16	0.90	-0.39	0.77	0.60	0.93
450	0.13	0.82	-0.59	0.69	0.50	0.76
500	0.36	0.76	-0.59	0.63	0.28	0.69
550	0.31	0.70	-0.54	0.61	0.27	0.64
600	0.17	0.66	-0.41	0.58	0.27	0.60
656.3	-0.02	0.62	-0.34	0.56	0.36	0.57
700	-0.13	0.59	-0.31	0.54	0.43	0.55
800	-0.23	0.54	-0.33	0.52	0.55	0.52
900	-0.21	0.49	-0.32	0.49	0.52	0.49
1000	0.03	0.51	-0.24	0.49	0.21	0.48
1050	0.21	0.53	-0.29	0.50	0.09	0.50
1200	0.35	0.66	-0.32	0.52	0.03	0.57
1550	0.92	0.78	-0.56	0.62	-0.28	0.81
1700	1.08	0.85	-0.56	0.69	-0.54	1.05
2100	0.61	0.97	0.03	0.77	-0.78	1.18
2300	-0.02	1.04	0.22	0.89	-0.27	1.22
2400	-0.22	1.08	0.31	0.95	-0.14	1.26
2500	0.06	1.13	0.51	1.07	-0.70	1.34

Figure 6-1, Figure 6-2, and Figure 6-3 show differences from the RV and their uncertainties of participants: KRISS, NIM, and VNIIOFI, respectively.

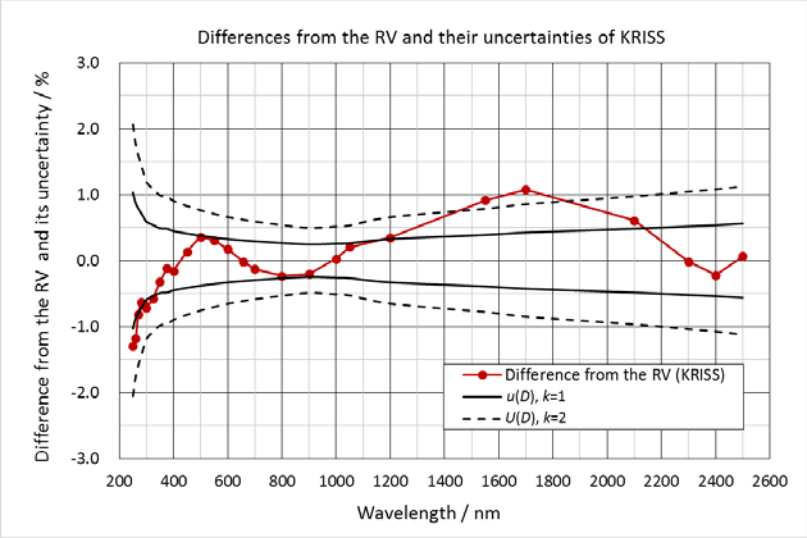

Figure 6-3. Differences from the RV and their uncertainties of KRISS.

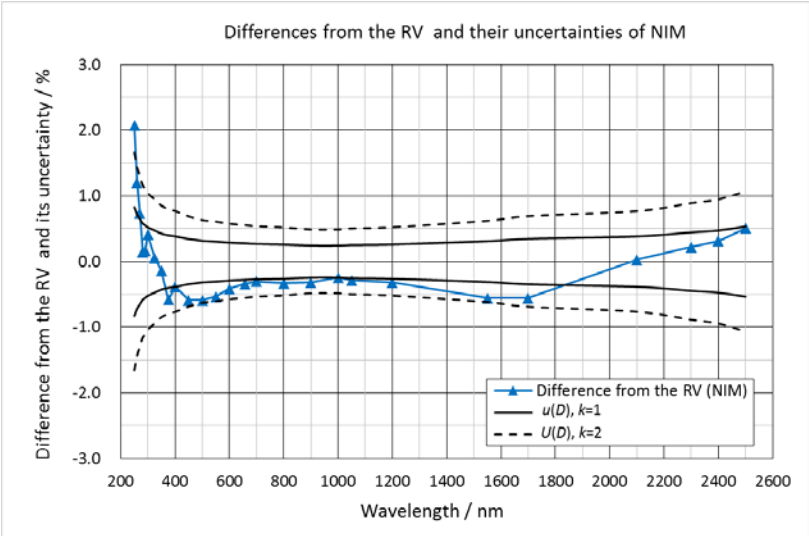

Figure 6-4. Differences from the RV and their uncertainties of NIM.

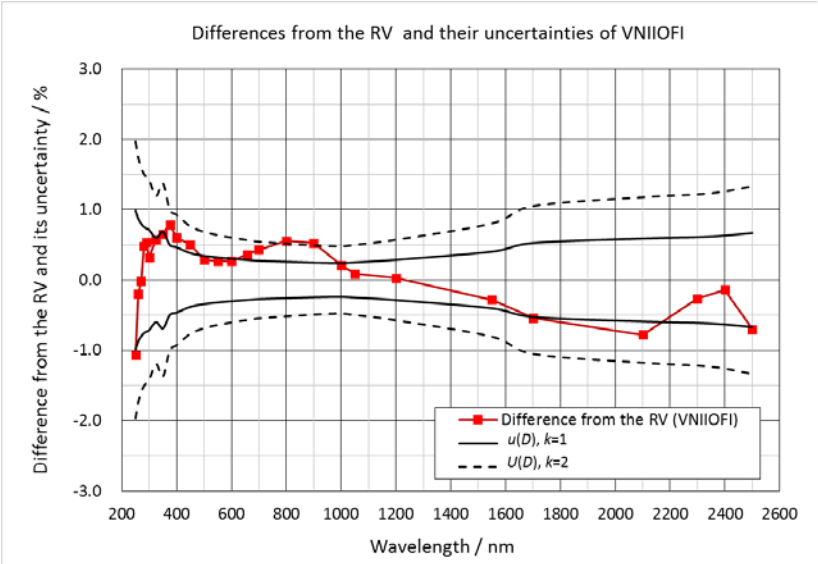

Figure 6-5. Differences from the RV and their uncertainties of VNIIOFI.

7. Conclusion

Korea Research Institute of Standards and Science (KRISS), National Institute of Metrology (NIM), and All-Russian Research Institute for Optical and Physical Measurements (VNIIOFI) conducted an international comparison on the spectral radiance over the spectral region from 250 nm to 2500 nm from 2013 to 2016. The aim of this comparison was to assess the equivalence of the spectral radiance scales between the three laboratories. The difference from the RV and its uncertainty of each participant of this comparison were calculated by using the relative difference model recommended by the Guidelines for CCPR Comparison Report Preparation. A method (Ratio Method) to calculate the difference from the RV and its uncertainty was proposed to eliminate the pilot effects involved in the relative difference model. In the Ratio Method, spectral radiance ratios to the pilot and geometric means were used to calculate the difference from the RV and it uncertainty of each participant. Results of this comparison analyzed using the Ratio Method showed that differences from the RV of all participants were within their uncertainties (k=2) except a few wavelengths for each participant.

8. References

[1] CCPR Working Group on Key Comparison, Guidelines for CCPR Key Comparison Report Preparation, CCPR-G2 Rev-3, July 1, 2013.

[2] B.B.Khlevnoy *et al*, CCPR-S1Supplementary comparison for spectral radiance in the range of 220 nm to 2500 nm, Metrologia, 46, S174-S180, 2009.

[3] E Woolliams E.R., Fox N.P., Cox M.G., Harris P.M., Harrison N.J., Final report on CCPR K1-a: Spectral irradiance from 250 nm to 2500 nm, *Metrologia*, **43**, *Tech. Suppl*. 02003, 2006.

[4] S.N. Park, C.W. Park, D.H. Lee, and B.H. Kim,"Consistency of the Temperature Scales above the Silver Freezing Point Realized at Four Different Spectral Bands," SICE-ICASE International Joint Conference 2006 Oct. 18-21, 2006 in Bexco, Busan, Korea (2006).

[5] Preston-Thomas H., "The International Scale of 1990 (ITS-90)," *Metrologia*, **27**, 3-10, 1990.

[6] JCGM 100:2008, Joint Committee for Guides in Metrology (September 2008), Evaluation of Measurement Data — Guide to the expression of uncertainty in measurement (GUM).

[7] Dai Cai-hong, Wu Zhi-feng, Yu Jia-lin. Realization of the new national primary scale of spectral radiance and spectral irradiance. *Proceedings of SPIE - The International Society for Optical Engineering*, v 8910, 2013, *International Symposium on Photoelectronic Detection and Imaging 2013: Imaging Spectrometer Technologies and Applications*. Vol.8910, Article number. 89100D-1.

[8] Dai Cai-hong, Wu Zhi-feng, Wang Yan-fei. Spectral radiance characterization and realization based on high temperature blackbody BB3500M. *Proceedings of SPIE - The International Society for Optical Engineering*, v 9795, 2015. Article number: 979527.

[9] S.A. Ogarev, B.B. Khlevnoy, M.L. Samoylov, V.I. Shapoval, V.I. Sapritsky, *in Proceedings of TEMPMEKO 2004, 9th International Symposium on Temperature and Thermal Measurements in Industry and Science*, ed. by D. Zvizdić, L. G. Bermanec, T. Veliki, T. Stašić (FSB/LPM, Zagreb, Croatia, 2004), pp. 569–574

[10] Samoylov M., Ogarev S., Khlevnoy B., Khromchenko V., Mekhontsev S. and Sapritsky V., High accuracy radiation TSP-type thermometers for radiometric scale realization in the temperature range from 600 to 3200 °C, *AIP Conference Proceedings* 684, 2003, pp. 583-588.

[11] http://www.kayelaby.npl.co.uk/general_physics/2_5/2_5_7.html

[12] A.V. Prokhorov, Monte Carlo method in optical radiometry, *Metrologia*, 1998, **35**, 465-471.

[13] V.I. Sapritsky and A.V. Prokhorov, Spectral effective emissivities of nonisothermal cavities calculated by the Monte Carlo method, *Appl. Opt.* **34**, 5645–5652 (1995).

[14] B.B. Khlevnoy, Metrological investigation of pyrographite high-temperature blackbodies, *Measurement Techniques*, Vol. 44, No. 12, 2001.

[15] S.G. Yousef, P. Sperfeld and J Metzdorf, Measurement and calculation of the emissivity of a high-temperature black body, *Metrologia*, 2000, **37**, 365.

[16] H.W. Yoon, C.E. Gibson and P.Y. Barnes, Realization of the NIST detector-based spectral irradiance scale, *Appl. Opt.* vol. **41**, N 28, 5879–5890 (2002).

[17] E. Woolliams et al., Thermodynamic temperature assignment to the point of inflection of the melting curve of high-temperature fixed points, *Philosophical Transactions of the Royal Society A*, p. 374: 20150044, 2015.

Appendix A. Ratio Method: A calculation method for the relative difference model

The Reference Value (RV) of this comparison was calculated basically in accordance with the Guidelines for CCPR Comparison Report Preparation (CCPR Key Comparison Working Group; CCPR-G2 Rev.3, July 1, 2013) [1]. Some problems, however, were found in calculations of uncertainties of relative differences, the uncertainty of the KCRV, DoE, and uncertainty of DoE for the relative difference model described in the Appendix B of the Guidelines. The first problem is that relative uncertainties of participants were used in the Appendix B. But uncertainties used in the calculation of the relative difference should be spectral irradiance uncertainties of participants relative to irradiances measured by the pilot, not to their own. The second one is that the effect of spectral irradiance measured by the pilot is remained in DoEs of participants. This means that DoEs of participants in a comparison depend on which NMI becomes the pilot.

In this appendix A, a calculation method of DoE (Ratio Method) is proposed for the relative difference model. The Ratio Method is similar to the method used in the Final Report of CCPR key comparison CCPR K1.a [3]. Spectral irradiance ratios of participants to the pilot and geometric means, however, were used to calculate DoEs and their uncertainties, instead of the systematic factor used in the Ref [3]. Problems found in Ref [1] and the details of Ratio Method proposed are described below.

A1. Problems found in calculations of DoE and its uncertainty in the appendix B of the Guidelines for CCPR Comparison Report Preparation [1]

1) A problem in the calculation of uncertainty of relative difference

Relative difference in the Guidelines is given by

$$\Delta_{i,j} = \frac{E_{i,j}}{E_{i,j}^{\mathrm{P}}} - 1. \qquad \text{Eq. (4) of Ref [1]}$$

And its uncertainty by

$$u(\Delta_{i,j}) = \sqrt{u_{\mathrm{rel}}^2(\overline{E}_{i,j}) + u_{\mathrm{rel}}^2(E_{i,j}^{\mathrm{P}}) + u_{\mathrm{rel,add}}^2(E_{i,j})} \qquad \text{Eq. (5) of Ref [1]}$$

But, from Eq. (4) of Ref [1], the uncertainty, $u(\Delta_{i,j})$ should be given as

$$u(\Delta_{i,j}) = \sqrt{\frac{u^2(\overline{E}_{i,j})}{\left(E_{i,j}^{\mathrm{P}}\right)^2} + \left(\frac{\overline{E}_{i,j}}{\left(E_{i,j}^{\mathrm{P}}\right)^2}\right)^2 u^2(E_{i,j}^{\mathrm{P}}) + u_{\mathrm{rel,add}}^2(E_{i,j})} \qquad \text{(A1-1)}$$

using absolute uncertainties and irradiance values instead of relative ones. And it can be given by

$$u(\Delta_{i,j}) = \sqrt{\left(\frac{\left(\overline{E}_{i,j}\right)^2}{\left(E_{i,j}^{\mathrm{P}}\right)^2}\right) \cdot \{u_{\mathrm{rel}}^2(\overline{E}_{i,j}) + u_{\mathrm{rel}}^2(E_{i,j}^{\mathrm{P}})\} + u_{\mathrm{rel,add}}^2(E_{i,j})} \qquad \text{(A1-2)}$$

with relative uncertainties. However, it is different from Eq. (5) of Ref [1]. Eq. (5) of Ref [1] is the relative uncertainty of $\left(\frac{E_{i,j}}{E_{i,j}^{\mathrm{P}}}\right)$.

In order for the uncertainty, $u(\Delta_{i,j})$ to be Eq. (5) of Ref [1], $u(\Delta_{i,j})$ should be replaced by $u_{\mathrm{rel}}(\Delta_{i,j})$ given by

$$u_{\mathrm{rel}}(\Delta_{i,j}) = \frac{u(\Delta_{i,j})}{1+\Delta_{i,j}} \qquad \text{(A1-3)}$$

2) A problem in the calculation of DoE

The KCRV, Δ_{KCRV} is given by

$\Delta_{\mathrm{KCRV}} = \sum_{i=0}^{N} w_i \Delta_i$ Eq. (17) of Ref [1]

and the unilateral DoE is given by

$D_i = \Delta_i - \Delta_{\mathrm{KCRV}}$. Eq. (21) of Ref [1]

By the definition of KCRV in Ref [1], The KCRV can be written as

$\Delta_{\mathrm{KCRV}} = \frac{E_{\mathrm{ref}}}{E^{\mathrm{P}}} - 1$, (A1-4)

using the reference value, E_{ref} and the pilot measurement result, E^{P} of a virtual artifact.

Then, DoE is given by

$D_i = \left(\frac{E_i}{E_i^{\mathrm{P}}} - \frac{E_{\mathrm{ref}}}{E^{\mathrm{P}}}\right)$. (A1-5)

Here, the pilot measurement effects like E_i^{P} and E^{P} are remained in the DoE, D_i of a participant *i*. In the relative difference model, however, the unilateral DoE of a participant *i* is defined as the difference between (a) the ratio of a typical measurement result of a participant to the reference value (virtual), and (b) its expected value of unity [3] given by

$D_i = \frac{X_i}{X_{\mathrm{ref}}} - 1$ for a measurand *X*. (A1-6)

Eq. (A1-5) used as DoE in Ref [1] is different from Eq. (A1-6) defined as DoE of the relative difference model.

A2. Ratio Method: A calculation method of the difference from the RV for the relative difference model

In this Appendix, Ratio Method proposed is specifically described and applied to obtain the difference from the RV for a spectral radiance comparison, as an example. Three lamps of the same type are assumed to be used as artifacts and measured by participants as well as the pilot. The spectral radiance of each lamp and its relative uncertainty are reported from each participant to the pilot. In this method, ratio of the spectral radiance measured by a participant to the spectral radiance measured by the pilot for each lamp is used instead of the systematic factor used in Ref [3], nor the relative difference used in Ref [1]. The mean ratio of a participant to the pilot is calculated by the geometric mean of three ratios for all lamps. The ratio of RV (Reference Value) to the pilot measurement (RV ratio hereinafter) is calculated by the weighted geometric mean of mean ratios of participants. Weights of participants are calculated by the same method recommended in Ref [1]. The difference from the RV and its uncertainty of each participant are calculated using the spectral radiance ratio of the participant and the RV ratio.

The following notations are used:

N	Number of participants, including the Pilot.
$L_{i,j}$	Spectral radiance of lamp *j* (=1 to 3) of a participant *i* measured by the participant.
$u_{rel}(L_{i,j})$	Relative uncertainty of $L_{i,j}$ reported by the participant *i*.
$L_{i,j}^{\mathrm{P}}$	Spectral radiance of lamp *j* of a participant *i* measured by the pilot.
$u_{rel}(L_{i,j}^{\mathrm{P}})$	Relative uncertainty of the pilot measurement, $L_{i,j}^{\mathrm{P}}$.
L_{ref}	Reference spectral radiance of the virtual artifact.

The spectral radiance ratio between the participant *i* and the pilot P is calculated as below.

$$r_{i,j} = \frac{L_{i,j}}{L_{i,j}^{\mathrm{P}}} \ , \tag{A2-1}$$

where $r_{i,j}$ is the spectral radiance ratio between a participant *i* and the pilot P, $L_{i,j}$is the spectral radiance of lamp *j* (*j* = 1, 2, 3) measured at the participant *i*, and $L_{i,j}^{\mathrm{P}}$is the spectral radiance of lamp *j* of the participant *i* measured at the pilot.
The relative uncertainty of the ratio $r_{i,j}$ is given by

$$u_{\mathrm{rel}}(r_{i,j}) = \frac{u(r_{i,j})}{r_{i,j}}. \tag{A2-2}$$

Then, it can be written as

$$u_{\mathrm{rel}}(r_{i,j}) = \sqrt{u_{\mathrm{rel}}^2(L_{i,j}) + u_{\mathrm{rel}}^2(L_{i,j}^{\mathrm{P}}) + u_{\mathrm{rel,add}}^2(L_{i,j})}, \tag{A2-3}$$

where $u_{\mathrm{rel,add}}(L_{i,j})$ is an additional uncertainty in the comparison for the lamp *j* of the participant *i* as defined in Ref [1].
For each lamp *j* at each participant *i*, when the participant measured twice, the mean spectral radiance of lamp *j* is defined as the geometric mean given by

$$\overline{L}_{i,j} = \left(\prod_{k=1}^{2} L_{i,j,k}\right)^{1/2}, \tag{A2-4}$$

then, its relative uncertainty can be calculated as the arithmetic mean of relative uncertainties of spectral radiances as below.

$$u_{\mathrm{rel}}(\overline{L}_{i,j}) = \frac{1}{2} \cdot \sum_{k=1}^{2} u_{\mathrm{rel},k}(L_{i,j}). \tag{A2-5}$$

Here uncertainty components of spectral radiance are assumed to be fully correlated between two measurements.
The mean ratio r_i for each participant

$$r_i = \left(\prod_{j=1}^{N} r_{i,j}\right)^{1/3}. \tag{A2-6}$$

Then, its relative uncertainty can be calculated as the arithmetic mean given by

$$u_{\mathrm{rel}}(r_i) = \frac{1}{3} \cdot \sum_{j=1}^{3} u_{\mathrm{rel}}(r_{i,j}), \tag{A2-7}$$

when the uncertainty components of three lamps measured by the participant *i* are assumed to be fully correlated.
The relative uncertainty of the mean ratio is given by

$$u_{\mathrm{rel}}(r_i) = \sqrt{u_{\mathrm{rel}}^2(\overline{L_i}) + u_{\mathrm{rel}}^2(\overline{L_i^{\mathrm{P}}}) + u_{\mathrm{rel,add}}^2(\overline{L_i})}. \tag{A2-8}$$

For the pilot laboratory (*i* =1 is used hereinafter),

$r_1 = 1$, $u_{\mathrm{rel}}(r_1) = 0$, and

$$u_{\mathrm{rel}}(\overline{L^{\mathrm{P}}}) = \frac{1}{3N} \cdot \sum_{i=1}^{N} u_{\mathrm{rel}}(\overline{L_i^{\mathrm{P}}}), \tag{A2-9}$$

where $u_{\mathrm{rel}}(\overline{L^{\mathrm{P}}})$ is the mean relative uncertainty of all measurements at the pilot laboratory.
The RV is calculated using weighted mean with cut-off. The cut-off value $u_{\mathrm{cut-off}}$ is calculated by

$$u_{\text{cut-off}} = \text{average}\,\{u_{\text{rel}}(\overline{L_i})\} \text{ for } u_{\text{rel}}(\overline{L_i}) \leq \text{median}\,\{u_{\text{rel}}(\overline{L_i})\}. \quad \text{(A2-10)}$$

The reported uncertainty $u_{\text{rel}}(\overline{L_i})$ of each participant *i* is adjusted by the cut-off

$$u_{\text{rel,adj}}(\overline{L_i}) = u_{\text{rel}}(\overline{L_i}) \text{ for } u_{\text{rel}}(\overline{L_i}) \geq u_{\text{cut-off}},$$

$$u_{\text{rel,adj}}(\overline{L_i}) = u_{\text{cut-off}} \text{ for } u_{\text{rel}}(\overline{L_i}) < u_{\text{cut-off}}. \quad \text{(A2-11)}$$

The adjusted uncertainty of the mean ratio $u_{\text{rel}}(r_i)$ after cut-off is given by

$$u_{\text{rel,adj}}(r_i) = \sqrt{u^2_{\text{rel,adj}}(\overline{L_i}) + u^2_{\text{rel,adj}}(\overline{L_i^{\text{P}}}) + u^2_{\text{rel,add}}(\overline{L_i})}. \quad \text{(A2-12)}$$

The ratio between the reference value L_{ref} and the pilot measurement L^{P} of a 'virtual reference' is given by

$$r_{\text{ref}} = \frac{L_{\text{ref}}}{L^{\text{P}}} \ . \quad \text{(A2-13)}$$

This ratio is the same as the reciprocal of the systematic factor of the pilot defined in Ref [3] given by

$$S_{\text{Pilot}} = \frac{L^{\text{P}}}{L_{\text{ref}}} \ . \quad \text{(A2-14)}$$

The Reference Value Ratio (RV ratio) in this Ratio Method is defined as the same as r_{ref}

$$r_{\text{RV}} = r_{\text{ref}} \quad \text{(A2-15)}$$

and is given by the weighted geometric mean of spectral radiance ratios to the pilot measurement as

$$r_{\text{RV}} = \prod_{i=1}^{N} r_i^{w_i} \quad \text{(A2-16)}$$

using the mean ratio and weight of each participant. This definition is equivalent to the constraint Eq. (17-7) of Ref [3] given by

$$\prod_{i=1}^{N} \left(\frac{L_i}{L_{\text{ref}}}\right)^{w_i} = 1. \quad \text{(A2-17)}$$

The weight w_i is determined by

$$w_i = u^{-2}_{\text{rel,adj}}(r_i) / \sum_{i=1}^{N} u^{-2}_{\text{rel,adj}}(r_i), \text{ then} \quad \text{(A2-18)}$$

$$\sum_{i=1}^{N} w_i = 1 \ . \quad \text{(A2-19)}$$

Since the mean ratio of the pilot is 1(one) and the sum of weight is 1(one), but the weight of the pilot is w_{P}, the RV ratio can be written as

$$r_{\text{RV}} = \frac{1}{\left(\overline{L^{\text{P}}}\right)^{1-w_{\text{P}}}} \prod_{i=2}^{N} (\alpha_i \overline{L_i})^{w_i}, i = 2, \cdots, N \text{ excluding the pilot} \quad \text{(A2-20)}$$

where normalizing constants α_i for each participant is used for normalization with the spectral radiance of pilot measurement $\overline{L^{\text{P}}}$ without changing the RV ratio.
The Chi-square value χ^2_{obs} for consistency check is given by

$$\chi^2_{\text{obs}} = \sum_{i=1}^{N} \frac{(r_i - r_{\text{RV}})^2}{u^2_{\text{rel,adj}}(r_i) \cdot r_i^2} \ . \quad \text{(A2-21)}$$

If $\chi^2_{\text{obs}} < \chi^2_{0.05}(\nu = N-1)$, then consistency is satisfied. $\chi^2_{0.05}(\nu)$ value is available from the table such as shown in the Appendix B of Ref [1].
The relative uncertainty of the RV ratio is given by

$$u_{\text{rel}}(r_{\text{RV}}) = \sqrt{\sum_{i=1}^{N} w_i^2 u_{\text{rel}}^2(\bar{L}_i) + (1-2w_{\text{P}})u_{\text{rel}}^2(\overline{L^{\text{P}}})}. \quad \text{(A2-22)}$$

The difference from the RV of a participant *i* is given by

$$D_i = \frac{r_i}{r_{\text{RV}}} - 1. \quad \text{(A2-23)}$$

It can be written as

$$D_i = \frac{L_i}{L_{\text{ref}}} - 1 \quad \text{(A2-24)}$$

as the definition of DoE, without any effect of the pilot measurement.
The relative uncertainty of $(1+D_i)$ is given

$$u_{\text{rel}}(1+D_i) = \frac{u(D_i)}{1+D_i} \ . \quad \text{(A2-25)}$$

The uncertainty of the difference from the RV of a participant *i* is given

$$\text{U}(D_i) = k \cdot (1+D_i) \cdot \sqrt{u_{\text{rel}}^2(r_{\text{RV}}) - (1-2w_{\text{P}})u_{\text{rel}}^2(\overline{L^{\text{P}}}) + (1-2w_i)u_{\text{rel}}^2(\bar{L}_i)} \ ; k=2. \quad \text{(A2-26)}$$

Note: Eq. (A2-26) takes into account the effect of correlation between r_i and r_{RV}. For any participant that is excluded from RV calculation, a simpler form applies:

$$\text{U}(D_i) = k(1+D_i) \cdot \sqrt{u_{\text{rel}}^2(r_{\text{RV}}) - (1-2w_{\text{P}})u_{\text{rel}}^2(\overline{L^{\text{P}}}) + u_{\text{rel}}^2(\bar{L}_i)} \ . \quad \text{(A2-27)}$$

End